# CONVERGENCE AND FUNCTIONAL EVOLUTION OF LONGIROSTRY IN CROCODYLOMORPHS

*by* ANTONIO BALLELL[1] (iD), BENJAMIN C. MOON[1] (iD), LAURA B. PORRO[1,2] (iD), MICHAEL J. BENTON[1] (iD) *and* EMILY J. RAYFIELD[1] (iD)

[1]School of Earth Sciences, University of Bristol, Life Sciences Building, 24 Tyndall Avenue, Bristol, BS8 1TQ, UK; ab17506@bristol.ac.uk, benjamin.moon@bristol.ac.uk, laura.porro@bristol.ac.uk l.porro@ucl.ac.uk, mike.benton@bristol.ac.uk, e.rayfield@bristol.ac.uk
[2]*Current address:* Department of Cell & Developmental Biology, UCL, Gower Street, London, WC1E 6BT, UK; l.porro@ucl.ac.uk

**Abstract:** During the Mesozoic, Crocodylomorpha had a much higher taxonomic and morphological diversity than today. Members of one particularly successful clade, Thalattosuchia, are well-known for being longirostrine: having long, slender snouts. It has generally been assumed that Thalattosuchia owed their success in part to the evolution of longirostry, leading to a feeding ecology similar to that of the living Indian gharial, *Gavialis*. Here, we compare form and function of the skulls of the thalattosuchian *Pelagosaurus* and *Gavialis* using digital reconstructions of the skull musculoskeletal anatomy and finite element models to show that they had different jaw muscle arrangements and biomechanical behaviour. Additionally, the relevance of feeding-related mandibular traits linked to longirostry in the radiation of crocodylomorph clades was investigated by conducting an evolutionary rates analysis under the variable rates model. We find that, even though *Pelagosaurus* and *Gavialis* share similar patterns of stress distribution in their skulls, the former had lower mechanical resistance. This suggests that compared to *Gavialis*, *Pelagosaurus* was unable to process large, mechanically less tractable prey, instead operating as a specialized piscivore that fed on softer and smaller prey. Secondly, innovation of feeding strategies was achieved by rate acceleration of functional characters of the mandible, a key mechanism for the diversification of certain clades like thalattosuchians and eusuchians. Different rates of functional evolution suggest divergent diversification dynamics between teleosaurids and metriorhynchids in the Jurassic.

**Key words:** feeding, convergence, finite element analysis, evolutionary rates, Crocodylomorpha, Thalattosuchia.

FEEDING is an essential biological function through which organisms incorporate nutrients and obtain energy. Consequently, feeding imposes strong selective pressure on vertebrate skull morphology (Wroe & Milne 2007; Jones 2008; Pierce *et al.* 2009). In an evolutionary context, feeding specialization can promote diversification by enabling the conquest of previously unexplored or newly available adaptive zones (Erwin 1992; Wainwright & Price 2016). Feeding specialisms may also promote niche partitioning whereby organisms coexist in the same ecosystem by using different food resources and different diets (Pierce *et al.* 2009; Button *et al.* 2014; Mallon & Anderson 2015). Therefore, characterizing feeding modes and diets is crucial when analysing evolutionary patterns.

Classical palaeontological work used anatomy as the main evidence to elucidate feeding and diet in fossil taxa. However, skull and dental morphology alone should not be used to test such inferences, as form and function are sometimes decoupled, especially in complex systems (Wainwright 2007). Modern morphofunctional and biomechanical techniques provide palaeontologists with a means to test functional hypotheses, aiming at overcoming the usual form-function mismatch. Finite element analysis (FEA) is a computational engineering technique that predicts the stress and strain in structures under certain loading conditions, making it suitable for modelling the effects of feeding forces on skulls (Rayfield 2007). FEA has been used extensively in recent years to test hypotheses of feeding mechanics in extinct taxa, including early tetrapodomorphs (Neenan *et al.* 2014), temnospondyls (Lautenschlager *et al.* 2016a), cynodonts (Gill *et al.* 2014), dinosaurs (Rayfield 2004, 2007; Button *et al.* 2014, 2016; Lautenschlager *et al.* 2016b; Taylor *et al.* 2017) and crocodylomorphs (Pierce *et al.* 2009; Young *et al.* 2010). Digital muscle reconstructions usually accompany FEA on extinct organisms to calculate jaw muscle forces that will serve as FEA input loads (Button *et al.* 2014, 2016; Lautenschlager *et al.* 2016b; Taylor *et al.* 2017). In fossil taxa, jaw muscles can be reconstructed with the identification of osteological correlates of muscle attachment and the use of homology criteria based on the extant

phylogenetic bracket (EPB; Witmer 1995). These techniques are particularly powerful when convergence is tested between fossil taxa and modern analogues, although such comparative studies are scarce for reptiles (Rayfield *et al.* 2007).

Feeding in fossil taxa has been analysed in a broader context by quantifying functional disparity through time, in a similar way to morphological disparity studies (Foote 1994; Wills *et al.* 1994; Brusatte *et al.* 2008; Thorne *et al.* 2011), including characters of the skull that are relevant to feeding mechanics (Anderson *et al.* 2013). Morphospaces of functional traits have been used to address feeding evolution, diversification and extinction events in different fossil clades such as placoderms (Anderson 2009), early tetrapodomorphs (Anderson *et al.* 2013), marine reptiles (Stubbs & Benton 2016), dinosaurs (Button *et al.* 2017; MacLaren *et al.* 2017) and crurotarsans (Stubbs *et al.* 2013).

Crocodylomorpha are the clade of crurotarsan archosaurs that include extant crocodiles and their closest extinct relatives (Brusatte *et al.* 2010). This lineage originated in the Carnian (Late Triassic), with their closest sister groups dating from the Ladinian to Carnian (Benton & Walker 2002; Butler *et al.* 2014). Soon after the origin of the clade, basal crocodylomorphs already exhibited a remarkable spectrum of skull morphologies suggesting disparate feeding modes (Irmis *et al.* 2013). Crocodylomorphs radiated throughout the Jurassic and Cretaceous, with many lineages occupying diverse ecological niches on land, in the sea and in semiaquatic environments (Bronzati *et al.* 2015), although most of these clades were wiped out by the Cretaceous–Palaeogene mass extinction (Kellner *et al.* 2014). Extant crocodiles are included in the eusuchian clade Crocodylia (Lee & Yates 2018), with a functional diversity representing a limited proportion of the feeding disparity of extinct crocodylomorphs (Stubbs *et al.* 2013). The conquest of the semiaquatic apex predator niche by this lineage was facilitated by the acquisition of a derived musculoskeletal anatomy of the skull that enabled the production of spectacular bite forces (Erickson *et al.* 2012) while keeping a hydrodynamically efficient profile (Busbey 1995; McHenry *et al.* 2006). Among extant crocodilians, the Indian gharial (*Gavialis gangeticus*) has the most specialized feeding habits, being a mostly piscivorous species that catches agile prey by fast sweeps of the head (Thorbjarnarson 1990).

Thalattosuchia were a highly successful lineage and key components of Mesozoic marine ecosystems. In the Early Jurassic, the functional disparity of crocodylomorphs escalated remarkably (Stubbs *et al.* 2013), caused by the radiation of thalattosuchians in the marine realm (Bronzati *et al.* 2015). This group became fully adapted to the marine environment and split into two clades, Teleosauridae and Metriorhynchidae (Young *et al.* 2010), which evolved divergent feeding habits and ecologies. Teleosaurs, mainly Early Jurassic forms with long snouts, pointed teeth and conservative body plan, have long been presumed to share a similar ecology and diet with the Indian gharial; that is, catching fish using lateral sweeps of the heads (Massare 1987; Hua & de Buffrenil 1996; Pierce *et al.* 2009). Metriorhynchids diversified in the Middle Jurassic and evolved further adaptations to a pelagic life, including the loss of osteoderms, modification of limbs into fins and a caudal fin (Young *et al.* 2010).

Longirostry, defined as the anteroposterior elongation of the snout, evolved independently in several crocodylomorph lineages such as thalattosuchians and eusuchians (Fig. 1). The evolution of longirostry is determined by a trade-off, as the mechanical vulnerability of long and slender snouts limits bite force production while the speed of attack and prey capture is increased (Taylor 1987), associated with a diet of soft and fast-moving prey like fish. Additionally, the associated elongation of mandibular symphyses imposes a constraint on prey size in long-snouted species (Walmsley *et al.* 2013). In line with biomechanical evidence, a recent study demonstrates that the convergent evolution of long snouts in crocodilians and river dolphins was driven by dietary specialization (McCurry *et al.* 2017*a*). These ideas led to the interpretation of many extinct longirostrine taxa as piscivores. One such taxon is the basal teleosaurid *Pelagosaurus typus* from the Early Jurassic, whose ecology and feeding habits have been interpreted as convergent with *Gavialis* (Pierce & Benton 2006), although no biomechanical analysis has tested this hypothesis.

Here, we explore the importance of feeding specialization in Crocodylomorpha throughout the Mesozoic and in the present. First, we test the hypothesis that the skulls of two longirostrine taxa (*Pelagosaurus* and *Gavialis*) respond similarly to feeding-induced loads, suggesting similar feeding mechanisms and dietary habits. To test this hypothesis, jaw muscle reconstruction and FEA are performed on 3D models of the two taxa to assess differences in stress distribution within their skulls. This research yields the first digital muscle reconstruction for a thalattosuchian and the first complete FE model for both taxa. Second, we assess the influence of changes in mandibular function and feeding through time in the macroevolution of Crocodylomorpha, making use of Bayesian phylogenetic methods to calculate rates of evolution of two mandibular characters.

*Anatomical abbreviations.* mAMES, musculus adductor mandibulae externus superficialis; mAMEM, musculus adductor
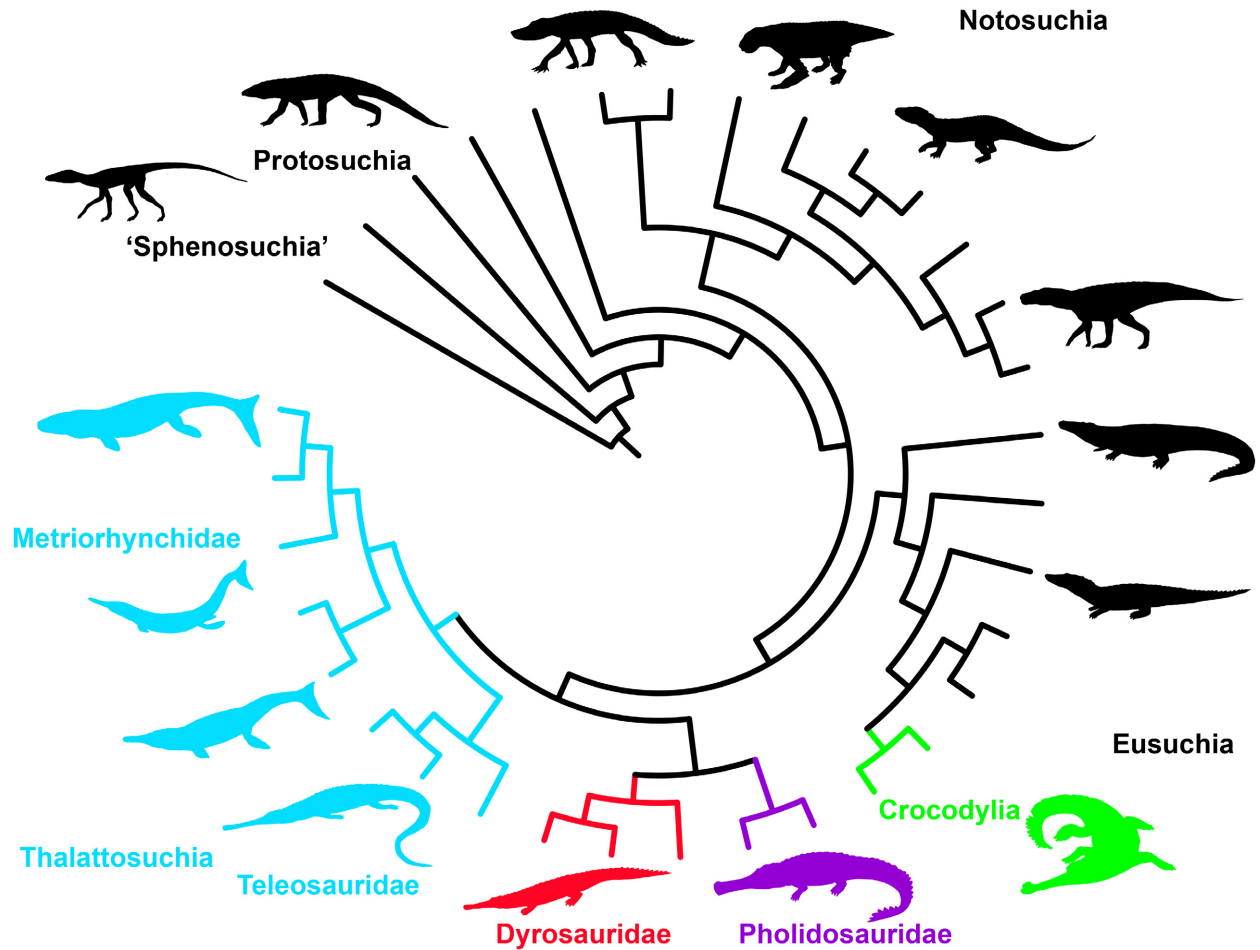
**FIG. 1.** Occurrences of longirostry in Crocodylomorpha. Phylogeny of major crocodylomorph clades, highlighting clades in which longirostry has evolved at least once: Eusuchia; Pholidosauridae; Dyrosauridae; Thalattosuchia. Colour online.

mandibulae externus medialis; mAMEP, musculus adductor mandibulae externus profundus; mAMP, musculus adductor mandibulae posterior; mIM, musculus intramandibularis; mPSTs, musculus pseudotemporalis superficialis; mPSTp, musculus pseudotemporalis profundus; mPTd, musculus pterygoideus dorsalis; mPTv, musculus pterygoideus ventralis.

## MATERIAL AND METHOD

*Segmentation and 3D model creation*

The specimen of *Pelagosaurus typus* used in this work is BRLSI M1413 (Fig. 2A), from the Toarcian (Early Jurassic) locality of Strawberry Bank in Ilminster, Somerset, England (Williams *et al.* 2015). This fossil is a sub-adult, with a skull 31 cm in length from the tip of the snout to the end of the retroarticular process (Pierce & Benton 2006). It was scanned by BCM in the Nikon XT H 225ST μCT scanner at the Life Sciences Building, University of Bristol (Ballel *et al.* 2019; scan parameters 210 kV, 130 μA, 27.3 W, 0.5 mm copper filter, 1 s exposure time, no binning, ultrafocus reflection target, 3141 projections and two frames per projection). The fossil was scanned in two parts and the scan data were joined in VGStudio Max v2 (Volume Graphics GmbH; https://www.volumegraphics.com). The CT data consists of 3419 slices of 0.0956 mm pixel size and 0.0956 mm thickness. *Gavialis gangeticus* specimen NHMUK 2005.1605 is an 86-cm-long skull of an extant adult gharial (Fig. 2B). It was scanned in a medical scanner at the Royal Veterinary College in London, with parameters set to 120 kV, 200 mA, field of view 320 × 320 pixels, yielding 161 slices of the cranium and 182 of the mandible, both 5 mm thick with a pixel size of 0.625 mm.

The CT data were segmented using Avizo Lite v9.4 (FEI Visualization Science Group; https://www.thermofisher.com) to generate virtual 3D models of the skulls. The anatomy of *Pelagosaurus* has been thoroughly
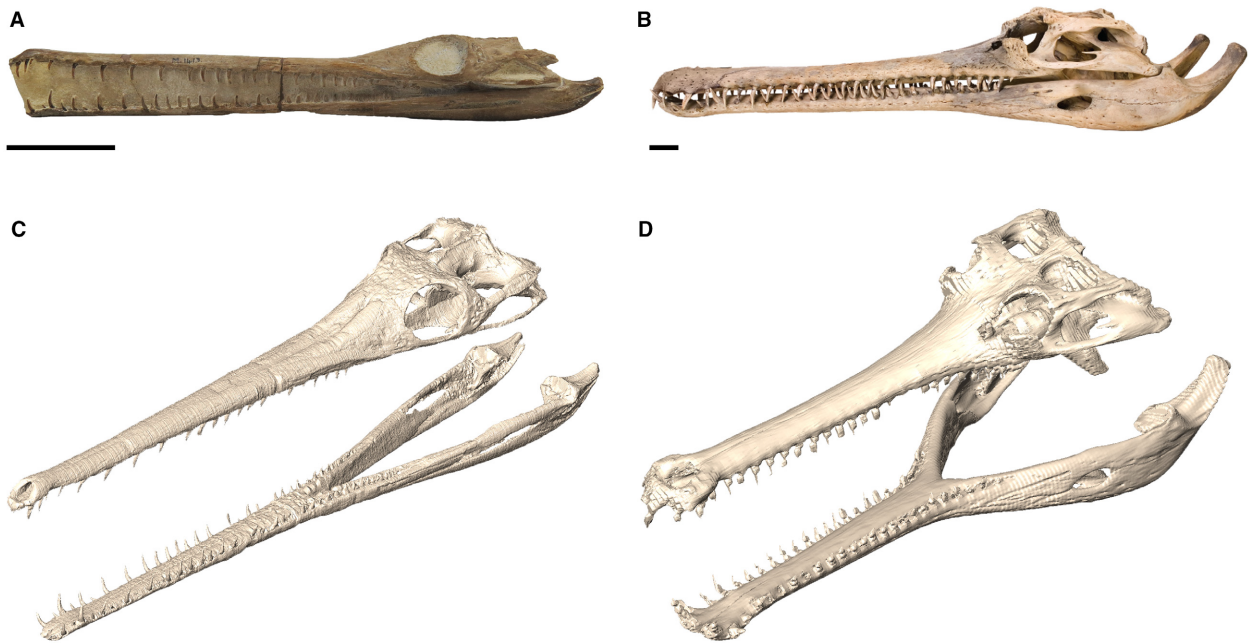
**FIG. 2.** Specimens and digital 3D models of *Pelagosaurus typus* and *Gavialis gangeticus*. A, *Pelagosaurus typus*, specimen BRLSI M1413, skull in right lateral view. B, *Gavialis gangeticus*, specimen NHMUK 2005.1605, skull in right lateral view, taken from Cuff & Rayfield (2013). C, reconstructed 3D model of *Pelagosaurus* after performing digital restoration of the fossil. D, segmented skull of *Gavialis gangeticus*, NHMUK 2005.1605. Scale bars represent 5 cm. Colour online.

described (Pierce & Benton 2006, Pierce *et al.* 2017), although the use of CT scanning enabled us to study bones that were previously unknown, such as the braincase and the medial elements of the mandible. The skull of *Pelagosaurus* was digitally reconstructed by labelling individual bones of the left side of the skull in the segmentation editor (Fig. 3). This side is better preserved than the right; therefore, left side elements were mirrored and merged to create bilaterally symmetric models of the cranium and the mandible (Fig. 2C). Taphonomic distortion was repaired

following a protocol for digital restoration of fossils (Lautenschlager 2016), including the removal of cracks using automatic interpolation. The gharial skull models did not require any restoration (Fig. 2D).

*Muscle reconstruction*

The skull models served as the bases for digital reconstructions of the jaw adductor musculature. Skulls of both
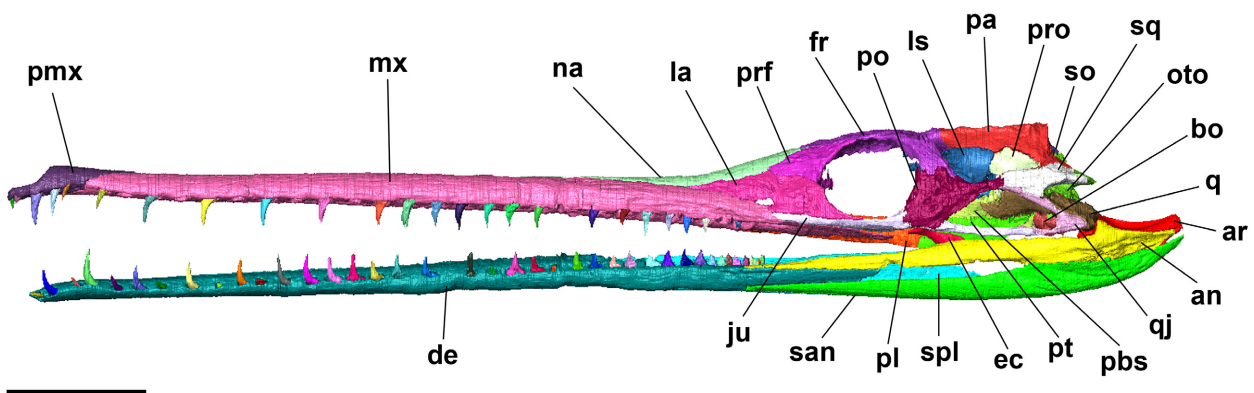


**FIG. 3.** Osteological reconstruction of *Pelagosaurus* BRLSI M1413. *Abbreviations:* an, angular; ar, articular; bo, basioccipital; de, dentary; ec, ectopterygoid; fr, frontal; ju, jugal; la, lacrimal; ls, laterosphenoid; mx, maxilla; na, nasal; oto, otoccipital; pa, parietal; pbs, parabasisphenoid; pl, palatine; pmx, premaxilla; po, postorbital; prf, prefrontal; pro, prootic; pt, pterygoid; q, quadrate; qj, quadratojugal; so, supraoccipital; san, surangular; spl, splenial; sq, squamosal. Scale bar represents 5 cm. Colour online.

species were examined for osteological correlates of muscle attachments. Jaw muscle descriptions of extant crocodilians (Iordansky 1964, 2011; Endo *et al.* 2002; Holliday & Witmer 2007; Holliday *et al.* 2013; Sellers *et al.* 2017) and a muscle reconstruction of the teleosaurid thalattosuchian *Steneosaurus brevior* (Mueller-Töwe 2006) served as guides to identify muscle attachment sites in *Pelagosaurus*. Three additional *Pelagosaurus* specimens, ranging from juveniles to adults, in the BRLSI (M1416, M1418 and M1420) were also examined, in addition to the study specimen. Muscle attachment sites in *Gavialis* were established by examining NHMUK 61.4.1.2, as well as reviewing published anatomical studies of crocodilian jaw muscles. Endo *et al.* (2002) describe the cranial myology of three extant longirostrine crocodilians, including *G. gangeticus*, although the specific attachment sites are not specified. However, the apomorphic jaw muscle traits of the gharial (e.g. mPTv not extending to the lateral surface of the retroarticular process and mPSTs being remarkably bulky) were incorporated into our reconstruction.

Eight jaw adductor muscles were modelled in Avizo following a protocol for digital muscle reconstruction (Lautenschlager 2013). Point to point connections (beams) were created from the muscle origin to the insertion sites, followed by fleshing out the muscles reflecting the spatial constraints imposed by the surrounding bones and muscles. Fleshing out the mPTv required more caution as it is not spatially constrained by the size of the adductor chamber or other muscles. Therefore, 3D digital muscle reconstruction of a juvenile *Alligator mississippiensis* (Holliday *et al.* 2013), dissections of modern crocodiles (Iordansky 1964, 2011) and photographs of living gharials were consulted to define the three-dimensional extent of this muscle in both taxa.

The cartilago transiliens, a cartilaginous element that acts as the origin and insertion point of some jaw adductors (Tsai & Holliday 2011), was not modelled here, following previous muscle reconstructions in extant crocodilians (Holliday & Witmer 2007; Sellers *et al.* 2017). Instead, the mPSTs and the mIM were considered as a single muscle complex (mPSTs) extending from the mPSTs origin site to the mIM insertion surface. This alternative was chosen because the presence of this characteristic element of extant crocodiles cannot be inferred with certainty in *Pelagosaurus* and it simplifies muscle modelling without affecting muscle volume calculations significantly. Further, the cartilago transiliens acts as a link between mPSTs and mIM, with collagenous fibres running from one muscle to the other and a cartilaginous disk connecting them (Tsai & Holliday 2011). Consequently, the digital modelling chosen here does not differ much from the anatomical arrangement and mechanical behaviour of the complex.

Muscle forces were calculated using the anatomical cross-sectional area (CSA) and the isometric stress value ($\sigma$) of 0.3 N/mm$^2$. CSA is usually calculated as the ratio of the muscle volume (MV) and the muscle length (ML) (Thomason 1991). Muscle volumes were calculated using the material statistics module in Avizo. For each muscle, five length measurements were taken using the measuring tool in Avizo and the mean was used as the ML. Fibre length (FL) was used to calculate CSA instead of ML following previous biomechanical studies (Bates & Falkingham 2012, 2018). Muscle fibres can be up to a third of the length of the muscle and thus FL was calculated as ML/3, and CSA as MV/FL (Bates & Falkingham 2018). Finally, the individual muscle forces were summed to obtain the total muscle force applied on each side of the skull in the original specimens and in a *Gavialis* scaled to the skull length of BRLSI M1413 (Table 1).

*Finite element analysis*

The cranium and mandible surface models created in Avizo were imported into Hypermesh v14 (Altair Hyperworks; https://altairhyperworks.co.uk). Owing to the complexity of the models, the shrink wrap tool was employed to overcome meshing problems by reducing surface complexity. Meshing was performed using tetrahedral elements, and an element size of 0.5 mm was chosen for this step, considered to be sufficiently small to avoid convergence issues (Bright & Rayfield 2011). The resulting meshes were composed of 2 280 000 (cranium) and 1 500 000 (mandible) elements in the *Pelagosaurus* cranium and mandible, and 7 020 000 (cranium) and 3 730 000 (mandible) elements in the *Gavialis* (Ballell *et al.* 2019, table S1).

FE models were assigned material properties of crocodilian skull bone: Young's modulus 15 GPa, Poisson's ratio 0.29 (Zapata *et al.* 2010; Porro *et al.* 2011), which was modelled as homogeneous and isotropic. Although anisotropic material properties have proved to more accurately predict the biomechanical behaviour in FE models of crocodilians (Porro *et al.* 2011), employing isotropic and homogeneous properties for *Pelagosaurus* and *Gavialis* allowed for comparisons between both taxa and with previous FE models of crocodilian skulls (Walmsley *et al.* 2013; McCurry *et al.* 2017b).

The models were constrained in all degrees of freedom at the quadrate condyles and at the glenoid fossa, fixing 10 nodes per side (20 per model). Tooth constraints were applied to simulate bilateral bites at three points along the tooth row (anterior, middle and posterior). Additionally, unilateral bites at an anterior and posterior tooth positions were analysed. Each tooth was constrained by 5 nodes in dorsoventral translation and rotation. Bilateral

**TABLE 1.** Muscle force calculations in *Pelagosaurus typus* and *Gavialis gangeticus*.

| Muscle | MV (mm$^3$) | ML (mm) | FL (mm) | CSA (mm$^2$) | F (N) | RMF (%) |
|---|---|---|---|---|---|---|
| *Pelagosaurus typus* BRLSI M1413 | | | | | | |
| mAMES | 679.592 | 14.684 | 4.895 | 138.843 | 41.653 | 9.3 |
| mAMEM | 662.687 | 14.686 | 4.895 | 135.371 | 40.611 | 9.0 |
| mAMEP | 3278.645 | 34.010 | 11.337 | 289.207 | 86.762 | 19.3 |
| mAMP | 1592.936 | 26.900 | 8.967 | 177.651 | 53.295 | 11.8 |
| mPSTs | 1761.511 | 42.342 | 14.114 | 124.806 | 37.442 | 8.3 |
| mPSTp | 50.263 | 36.768 | 12.256 | 4.101 | 1.230 | 0.3 |
| mPTd | 6632.511 | 91.310 | 30.437 | 217.912 | 65.374 | 14.5 |
| mPTv | 6573.912 | 47.790 | 15.930 | 412.675 | 123.802 | 27.5 |
| | | | | Total | 450.170 | 100 |
| *Gavialis gangeticus* NHMUK 2005.1605 | | | | | | |
| mAMES | 52 527.852 | 72.844 | 24.281 | 2163.294 | 648.988 | 9.2 |
| mAMEM | 33 610.553 | 65.181 | 21.727 | 1546.955 | 464.086 | 6.6 |
| mAMEP | 161 698.515 | 121.571 | 40.524 | 3990.236 | 1197.071 | 17.0 |
| mAMP | 41 850.572 | 99.521 | 33.174 | 1261.566 | 378.470 | 5.4 |
| mPSTs | 108 700.988 | 166.909 | 55.636 | 1953.775 | 586.132 | 8.3 |
| mPSTp | 1576.694 | 136.150 | 45.383 | 34.742 | 10.423 | 0.1 |
| mPTd | 446 824.602 | 292.890 | 97.630 | 4576.716 | 1373.015 | 19.5 |
| mPTv | 438 120.968 | 166.249 | 55.416 | 7905.982 | 2371.795 | 33.7 |
| | | | | Total | 7029.979 | 100 |
| *Gavialis gangeticus* NHMUK 2005.1605 scaled to *Pelagosaurus* size | | | | | | |
| mAMES | 1939.270 | 24.942 | 8.314 | 233.254 | 69.976 | 9.2 |
| mAMEM | 1240.864 | 22.318 | 7.439 | 166.798 | 50.039 | 6.6 |
| mAMEP | 5969.729 | 41.626 | 13.875 | 430.240 | 129.072 | 17.0 |
| mAMP | 1545.077 | 34.076 | 11.359 | 136.026 | 40.808 | 5.4 |
| mPSTs | 4013.120 | 57.150 | 19.050 | 210.662 | 63.199 | 8.3 |
| mPSTp | 58.210 | 46.618 | 15.539 | 3.746 | 1.124 | 0.1 |
| mPTd | 16 496.268 | 100.286 | 33.429 | 493.477 | 148.043 | 19.5 |
| mPTv | 16 174.939 | 56.924 | 18.975 | 852.449 | 255.735 | 33.7 |
| | | | | Total | 757.996 | 100 |

All values correspond to only one side of the skull. CSA, anatomical cross-sectional area; F, muscle force (in N); FL, fibre length; ML, muscle length; MV, muscle volume; RMF, relative muscle force.

and unilateral bites represent different loading scenarios, with bending and torsion being the main loading regime acting on the models, respectively.

Finally, the calculated muscle forces were applied to the models. This was performed by choosing between 40 and 100 nodes covering the identified areas of muscle origin and insertion (except for mPSTp, which presents very restricted attachment areas that were sufficiently delimited by 5 nodes) and dividing the force magnitude by the number of chosen nodes. Force vectors were given the orientation of their corresponding muscles, as defined via a line from the origin to the insertion points. Models were loaded while keeping the same total muscle force to surface area ratio (Dumont *et al.* 2009) using *Pelagosaurus* muscle forces as reference, therefore scaling the models to compare shape and minimize the effects of size.

Hypermesh models were imported and analysed in Abaqus v6.14 (Dassault Systèmes Simulia; https://www.3ds.com). Contour plots were generated to highlight the distribution of von Mises stress, a metric that measures a

material's tendency to undergo ductile failure (Rayfield 2007; Dumont *et al.* 2009), in the cranium and mandible. Von Mises stress reflects the effect of both tension and compression on the skull and is the usual metric used to summarize FEA results. Median 95% von Mises stress values were calculated for all models in the anterior biting scenarios to compare the relative mechanical resistance of the skulls (Ballell *et al.* 2019, figs S1, S2). This method excludes the top 5% stress values, which may include anomalous stress recorded in elements close to constraints or with high aspect ratios (Walmsley *et al.* 2013; McCurry *et al.* 2017b).

*Evolutionary rates analysis of functional characters*

The anterior mechanical advantage (AMA) and size-corrected maximum jaw depth (MJD) were calculated in a sample of crocodylomorph species, following Anderson *et al.* (2013) and Stubbs *et al.* (2013). These two

continuously variable functional characters were selected as they describe different aspects of the mechanical performance of the mandible. AMA indicates the fraction of the jaw muscle force that is transformed into a bite force at the tip of the mandible and is measured as the in-lever/out-lever ratio (Ballell *et al.* 2019, fig. S3A). The in-lever was measured from the glenoid fossa (fulcrum) to the midpoint of the adductor muscle (mAME) insertion on the dorsal surface of the surangular and, in some taxa, the coronoid eminence. The out-lever was measured from the fulcrum to the base of the anteriormost tooth. MJD is a proxy to measure the resistance to dorsoventral bending of the mandible and is calculated by dividing the maximum jaw depth by jaw length (Ballell *et al.* 2019, fig. S3B). The lower jaws were oriented with the tooth row horizontal, with the maximum jaw depth measured perpendicular to it.

The taxa selected for the analysis consisted of two outgroups, *Gracilisuchus stipanicicorum* (Butler *et al.* 2014) and *Erpetosuchus granti* (Benton & Walker 2002), and 60 crocodylomorph species belonging to diverse lineages. The presence of well-preserved mandible material and image availability in the literature determined these choices. A database with pictures or reliable reconstructions of mandibles in lateral view (Ballell *et al.* 2019) was compiled from publications and from the NHMUK Data Portal (http://data.nhm.ac.uk/). Images were imported into ImageJ v1.51j8 (Schneider *et al.* 2012) to measure both characters. Taxon age ranges were downloaded from the Paleobiology Database (http://fossilworks.org/), covering a time span from the Ladinian (Middle Triassic) to the Eocene. Finally, an informal supertree of Crocodylomorpha was built by assembling published phylogenies of the clade. The relationships of basal crocodylomorphs ('Sphenosuchia') were based on Clark *et al.* (2004) and Irmis *et al.* (2013), and those of Protosuchia and non-mesoeucrocodylian crocodyliformes on Bronzati *et al.* (2012) and Buscalioni (2017). The phylogeny of Notosuchia was built following Pol *et al.* (2014) and Leardi *et al.* (2015), where Uruguaysuchidae is considered a clade and the sister group of Peirosauridae. The hypothesis of Bronzati *et al.* (2012) was used to build the phylogeny of Neosuchia, and a consensus of published phylogenetic analyses (Pierce *et al.* 2009; Young *et al.* 2010, 2012*a*, 2013) was used for Thalattosuchia.

A time-calibrated phylogeny was generated in R v3.4.2 (R Core Team 2017) from the cladogram and the age ranges, using the `ape` package (Paradis *et al.* 2004) and two calibration methods from the `timePaleoPhy` function in the `paleotree` package (Bapst 2012): the 'equal' method (Lloyd *et al.* 2012) with the time variable set as 2 myr, and the 'minimum branch length' method (Laurin 2004) with the time variable set as 1 myr. An additional scaling method, the fossilized birth–death model (Heath *et al.* 2014), was implemented in MrBayes v3.2.6

(Ronquist *et al.* 2012) using the function `cre-ateMrBayesTipDatingNexus` in `paleotree`, which follows the methods and suggestions from Matzke & Wright (2016). Taxa were sampled as point occurrences from uniform distributions bounded by their first and last occurrences apart from *Iharkutosuchus makadii*, which was fixed at 85.8 Ma to place the resulting tree in absolute time. Following the analysis in MrBayes, the Most Clade Credible Tree (MCCT) was extracted and placed into absolute time using the `paleotree` function `obtainDatedPosteriorTreesMrB`.

The time-scaled phylogenies and both raw and Z-transformed continuous measurements were analysed in BayesTraits v3.0.1 under the variable rates model (Venditti *et al.* 2011), a useful method to find rate shifts in clades that allows rates of evolution to change in time. A burnin of $10^7$ (9%) and $1.1 \times 10^8$ iterations were selected, and the output file was read in the online tool http://www.evolution.reading.ac.uk/VarRatesWebPP/ (Baker *et al.* 2016). Among the resulting parameters, mean rate scalar values were used to quantify the magnitude of evolutionary rates in each branch, while $\Delta_B$ and $\Delta_V$ were used to identify rate shifts along branches. These two parameters represent the gradual background rate of trait change and the rate of change which is not due to the background rate, respectively. Most importantly, the $\Delta_V/\Delta_B$ ratio was calculated for each node in the tree, with values higher than 2 taken as indicative of significant rate shifts and positive selection on that particular character (Baker *et al.* 2016). Randomization tests were conducted to identify significantly high and low mean rate scalar values in clades of interest (i.e. Thalattosuchia, Teleosauridae and Eusuchia). This was done by randomly sampling mean rate values in the same number of branches to the clade of interest, calculating the differences in means between sampled and non-sampled branches and replicating the process 9999 times. The true difference in mean rates was calculated in all replicates and divided by 10 000 to obtain the *p*-value (Ballell *et al.* 2019, figs S8, S9, table S3). Finally, mean rate values were plotted onto the time-scaled phylogeny using the `geoscalePhylo` function in the `strap` package (Bell & Lloyd 2015) and the `color.scale` function in the `plotrix` package (Lemon 2006) in R to identify branches where high and low rates of trait evolution occurred. Radiations and divergent macroevolutionary patterns in different clades are detected by rate shifts and maintained rate acceleration.

## RESULTS

*Jaw adductor anatomy and forces*

The supratemporal fossa was preserved in all specimens of *Pelagosaurus*, with the origin sites for mPSTs and

mAMEP visible on the anteromedial and posteromedial surfaces, respectively. The left quadrate was exposed in ventral view in BRLSI M1420, where the origin sites for mAMEM and mAMP were identified, separated by a distinctive crest. The origin of mPTv is present on the smooth posterior end of the pterygoid flanges, which are exposed in BRLSI M1413 and M1420. However, the only visible muscle insertion sites were those of mAMES and mPTv, located on the smooth dorsolateral surface of the surangular and the pitted lateral surface of the retroarticular process, respectively. The remaining attachment surfaces were missing or covered by sediment in all specimens, such as those of the medial bones of the mandible. In these cases, attachment sites were identified in the digital *Pelagosaurus* model and inferred by homology with extant crocodilians (Holliday & Witmer 2007; Sellers *et al.* 2017).

The reconstructed jaw adductor anatomy in *Pelagosaurus* (Fig. 4A–D) appears plesiomorphic to modern crocodilians (Fig. 4E–H), as expected by the EPB. The mAMES is the most superficial portion of the mAME and possesses a fan-shaped morphology with a nearly vertical orientation (Fig. 4A). The mAMEM is slightly smaller and is located medially and attaches to the dorsomedial surface
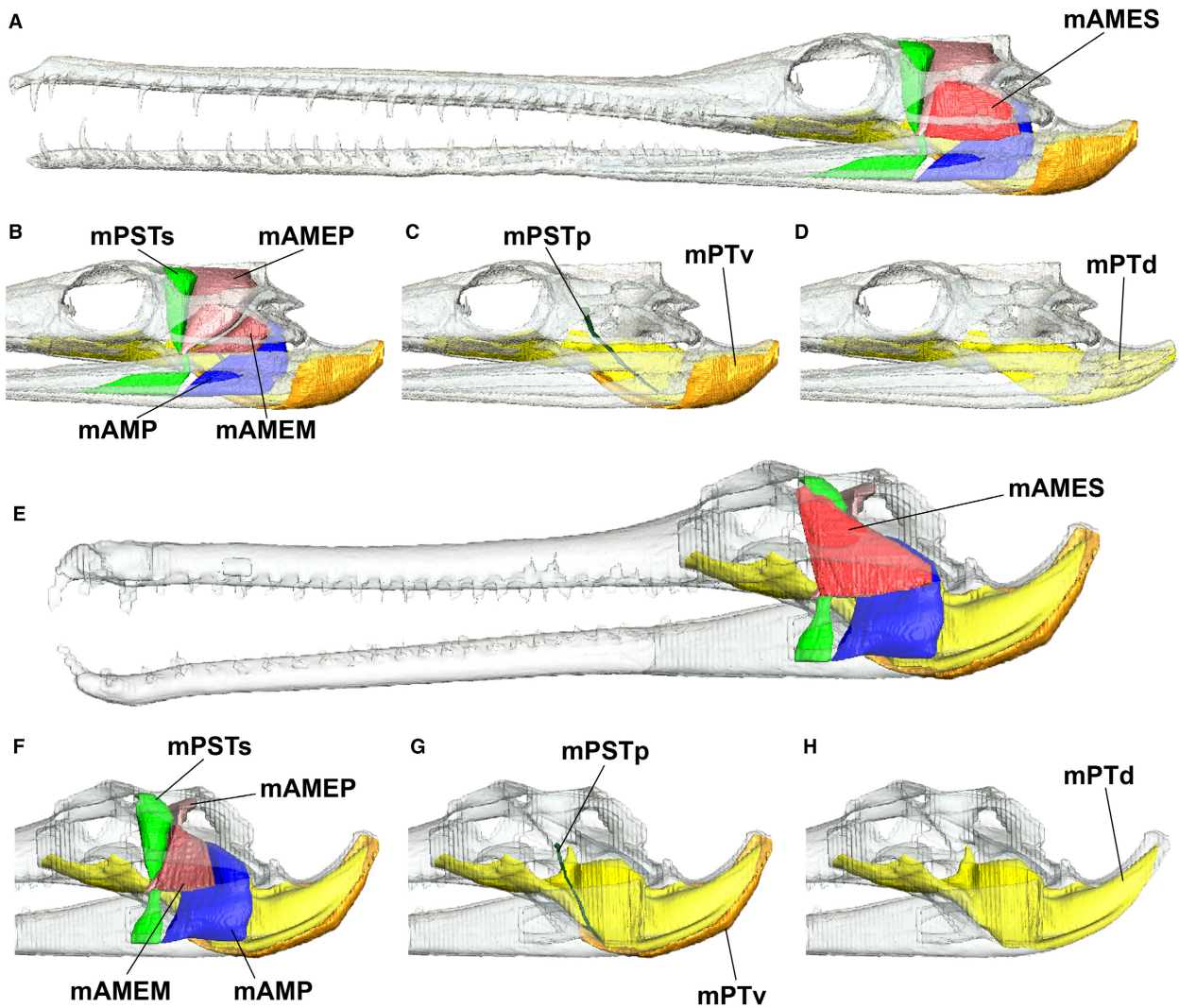


**FIG. 4.** Digital reconstruction of the jaw adductor musculature of *Pelagosaurus* (A–D) and *Gavialis* (E–H). A, E, skulls in lateral view showing all muscle complexes. B–D and F–H, digital dissection of jaw muscles after removing mAMES (B and F), mAMEM, mAMEP, mAMP and mPSTs (C and G) and mPSTp and mPTv (D and H). *Abbreviations:* mAMES, musculus adductor mandibulae externus superficialis; mAMEM, musculus adductor mandibulae externus medialis; mAMEP, musculus adductor mandibulae externus profundus; mAMP, musculus adductor mandibulae posterior; mPSTs, musculus pseudotemporalis superficialis; mPSTp, musculus pseudotemporalis profundus; mPTd, musculus pterygoideus dorsalis; mPTv, musculus pterygoideus ventralis. Colour online.

of the surangular (Fig. 4B). The mAMEP is a bulky muscle, the biggest within the adductor chamber, and occupies the posterior part of the supratemporal fossa (Fig. 4B). The mAMP is remarkably bulky and posterodorsally oriented in *Pelagosaurus*, is closely positioned to the jaw joint and inserts on the posterior part of the mandibular fossa (Fig. 4B). The mPSTs attaches to the anterior region of the supratemporal fossa, passes lateral to the pterygoid flange and its ventral ramus (mIM) occupies the anterior portion of the mandibular fossa (Fig. 4B). The mPSTp is an elongated and slender muscle that originates on the braincase and inserts on the posterolateral surface of the angular (Fig. 4C). The mPTd is a large and long muscle with anteroposterior orientation that courses dorsally to the posterior part of the palatines and the pterygoid flange and attaches to the medial surface of the retroarticular process (Fig. 4D). The mPTv is the bulkiest muscle in *Pelagosaurus* and it is oriented ventrolaterally (Fig. 4C). It covers the posteromedial surface of the mPTd and wraps around the posteroventral region of the retroarticular process, inserting on its lateral surface.

The relative patterns of force production for the different jaw muscle groups are consistent between *Pelagosaurus* and *Gavialis* (Table 1), with almost all forces being higher in the gharial even when the skulls are scaled to the same length. The mAME complex is responsible for 37.5% and 32.8% of the total muscle force in *Pelagosaurus* and *Gavialis*, respectively. While the relative importance of the mAMES in the total force is the same in both taxa, mAMEM and mAMEP forces represent a lower fraction of the total muscle force in *Gavialis*. Remarkably, the force produced by the mAMP is higher in *Pelagosaurus* than in *Gavialis*, in contrast to the relationship seen in the rest of muscles. This muscle exerts 11.8% of the total muscle force in the teleosaurid and 5.4% in the gharial. The force patterns for the mPST complex are very similar in the two taxa. This muscle group produces 9.6% and 9.5% of the total force in the thalattosuchian and the gharial, and most of those fractions are attributable to the mPSTs. Finally, mPT is the most powerful jaw adductor in terms of force production in both taxa, generating 42.0% of the total muscle force in *Pelagosaurus* and 53.3% in *Gavialis*. Of its two branches, mPTv is responsible for a greater fraction of the muscle force (27.5% and 33.7%, respectively). Overall, the jaw closing musculature of *Gavialis* exerts 7030 N, 15 times the force exerted by the jaw muscles of *Pelagosaurus* (450 N), presumably due to the notable size difference between the two specimens. When scaled to the same length, *Gavialis* jaw adductors still exert almost twice as much force as those of *Pelagosaurus* (758 N), demonstrating that the jaw closing muscles of the gharial are proportionately larger than those of *Pelagosaurus* and suggesting that the gharial skull is under significantly higher muscle

loads. Variation in MV is unlikely to result in substantially different force values considering the osteology, which largely constrains muscle anatomy in this area. Most muscles could only have minor changes in reconstructed volume while been kept anatomically feasible. Fibre length is a more arbitrary variable and could have greater influence on muscle force estimates. By changing FL to a fifth of ML muscle forces become on par with the scaled gharial, whereas a value of ML/47 is needed to achieve forces estimated for the full-size gharial forces, representing a 60% change in the gross muscle fibre length for each muscle. These values are unrealistic and suggest that *Pelagosaurus* jaw musculature could exert notably lower force than that of *Gavialis*.

*Patterns of stress distribution*

The stress distributions in the skulls of *Pelagosaurus* and *Gavialis* show some similarities in the bilateral biting scenario. During an anterior bilateral bite (Fig. 5), the dorsal surface of the snout (formed by the maxillae, the nasals and the anterior part of the frontals) is one of the cranial regions under highest stress. In both taxa, stresses higher than 10 MPa occur in the secondary palate formed by the maxilla, palatines and pterygoids. These high stress regions extend further anteroposteriorly in *Pelagosaurus*, in which a high stress patch appears around the fossa between the posterior portion of the nasals. High stresses are also located in the posterior part of the pterygoid flange, where mPTv originates, particularly in the gharial, in which this structure is more developed. As expected, the supratemporal fossae are under moderately high stresses in both taxa, and in *Pelagosaurus* stress in the posteroventral surface of this region is higher than 10 MPa. In *Pelagosaurus*, the slender infratemporal bar experiences high stress (Fig. 5A) in contrast to the more robust bar of *Gavialis* (Fig. 5B). The quadrates, bones that participate in the jaw joint and to which some jaw adductors attach, also show high stresses. The area around the frontoparietal suture concentrates high stress in *Pelagosaurus*. Cranial areas under low stress include the tip of the snout (premaxillae) and the occipital region. In *Pelagosaurus*, low stress also occurs in the posterior part of lacrimals and prefrontals, the middle part of the frontals and the ventral portion of the postorbital bar (Fig. 5A). In *Gavialis*, bones surrounding the infratemporal fenestra exhibit reduced stress (Fig. 5B). In general, more extensive areas of high stress are present in the *Pelagosaurus* cranium.

In the mandible, the stress distribution is consistent with the patterns seen in the cranium. Peak stresses over 10 MPa are located in the dorsal and ventral areas of the mandible that are adjacent to the symphysis. The lateral sides of the mandible show intermediate areas of stress in
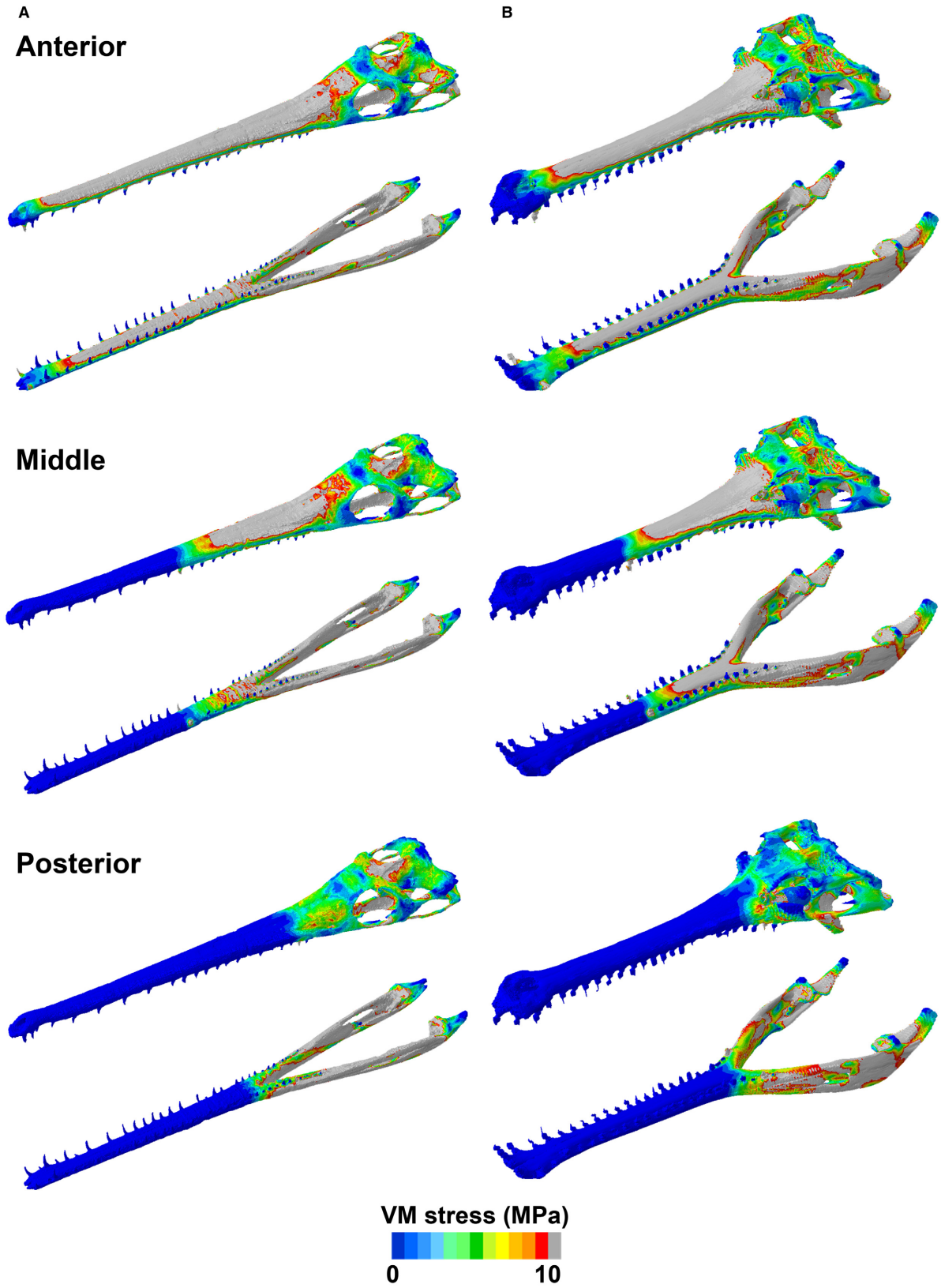
**FIG. 5.** Von Mises stress distribution plots of the skulls of *Pelagosaurus* (A) and *Gavialis* (B) simulating bilateral biting scenarios at anterior, middle and posterior tooth positions. Grey areas represent von Mises stress values higher than 10 MPa.

both taxa, and the posterior part of the symphysis exhibits higher stress in *Pelagosaurus* (Fig. 5A). The stress distribution along the postsymphyseal areas of the mandible differs in both taxa, with high stress found in *Pelagosaurus* and moderate to high stresses in *Gavialis*. The posterior end of the retroarticular process and the tip of the mandible are under low stress in both taxa, although in *Gavialis* low-stress regions extend further posteriorly along the mandible (Fig. 5B). Overall, the mandible of *Pelagosaurus* is under higher stress than that of *Gavialis*.

The middle and posterior bilateral bite scenarios yield different results from the anterior bite and stress distribution patterns are similar between both taxa, although differences are more pronounced during posterior bites (Fig. 5). In the cranium, the most remarkable difference is the stress magnitude experienced by the snout, which is very low in both taxa. The biting teeth mark the anterior extent of high stress areas, which is thus more posteriorly restricted in the posterior bite. Stress also decreases in the supratemporal fossae but increases around the infratemporal fenestrae. This is particularly evident in *Pelagosaurus*, in which stress around the supratemporal fossa decreases below 10 MPa. Other bones in which a reduction of stress levels occurs are the frontals and the braincase. Von Mises stress patterns in the pterygoid flanges and quadrates are similar to the anterior bite scenario in both taxa. In *Pelagosaurus*, the frontoparietal suture is under very high stresses in both scenarios, unlike the gharial. During a posterior bite, the high stress area in the dorsal part of the snout and the secondary palate seen in the anterior and middle bites disappear, and high stresses concentrate in the lacrimals and prefrontals. In the mandible, the symphyseal region anterior to the bite point is under minimal stress. There are no 10 MPa or higher stress areas in the symphyseal portion of the mandible during a posterior bite, unlike the other two scenarios. There is a slight decrease of stress in the postsymphyseal region, particularly in *Gavialis*, although areas of the dentary close to the bite point show a small increase in stress compared to the anterior bite. Therefore, stress acting on both the cranium and the mandible during a bite at middle and particularly posterior teeth is generally lower than at anterior teeth.

When simulating a unilateral bite at the tip of the snout, the von Mises stress distribution varies slightly compared to the bilateral scenario (Fig. 6). In both cranium and mandible, higher stresses extend more anteriorly towards the tip of the snout. Additionally, there is asymmetry in stress distribution in this region, with higher stresses shifting towards the working side (left). The most significant difference is seen in the lateral sides of the snout, where an increase in stress occurs in both taxa in the unilateral bite model. In contrast, the patterns of stress distribution in the posterior part of the cranium and the postsymphyseal region of the mandible are practically the same as in a bilateral anterior bite. There are no significant differences between *Pelagosaurus* and *Gavialis* in unilateral biting beyond those mentioned for bilateral biting.

During a unilateral posterior bite, the patterns of stress distribution in both taxa are similar to the bilateral scenario, although higher stresses are registered (Fig. 6). This is particularly evident in the lacrimals and prefrontals, which are under stress above 10 MPa. In *Gavialis*, the high-stress patch is located around the orbit while it extends further anteriorly in *Pelagosaurus* without contacting the orbit. The frontals also experience an increase in stress with respect to the bilateral posterior bite. The supratemporal fossa, the infratemporal bar and the quadratojugal seem to be under higher stress in *Gavialis*. In *Pelagosaurus*, higher stresses are present in the contralateral supratemporal fossa. The stress distribution in the mandibles is very similar to the bilateral scenario, with high stresses located in the postsymphyseal region.

Median von Mises stress is always higher in the lower jaw than the cranium for both taxa and decreases in both the upper and lower jaw as the bite point moves posteriorly (Ballell *et al.* 2019, figs S1, S2). One notable difference, however, is that stress is substantially lower in the gharial lower jaw than in that of *Pelagosaurus* in all bite scenarios. In contrast, there are far fewer discrepancies in stress values in the crania of both taxa and in a few cases the upper jaw of *Pelagosaurus* experiences slightly lower stress than that of the gharial. Therefore, it is the lower jaw of *Pelagosaurus* that is structurally weaker to feeding loads than the lower jaw of the gharial while the crania are similarly robust in both taxa.

*Evolutionary rates of functional characters*

Rates of evolution of AMA and MJD show different patterns through crocodylomorph phylogeny, with MJD being the more slowly evolving trait (Figs 7, 8). The highest rates of evolution in AMA are seen in Thalattosuchia for the three time-scaling methods (Fig. 7; Ballell *et al.* 2019, figs S4, S6, S8, S9, table S3), which exhibit low mechanical advantage compared to other crocodylomorph taxa. Within this clade, the increase in evolutionary rates is greater in teleosaurids than in metriorhynchids, especially in the fossilized birth–death tree, in which the latter exhibit intermediate to low rates (Ballell *et al.* 2019, fig. S6). Rate acceleration is particularly intense in the branch including *Machimosaurus* and *Steneosaurus*, the latter being the fastest evolving genus of all crocodylomorphs. *Pelagosaurus* has one of the lowest AMA among Thalattosuchia, with higher rates of evolution than metriorhynchids but lower than other teleosaurids. Other clades that exhibit high to
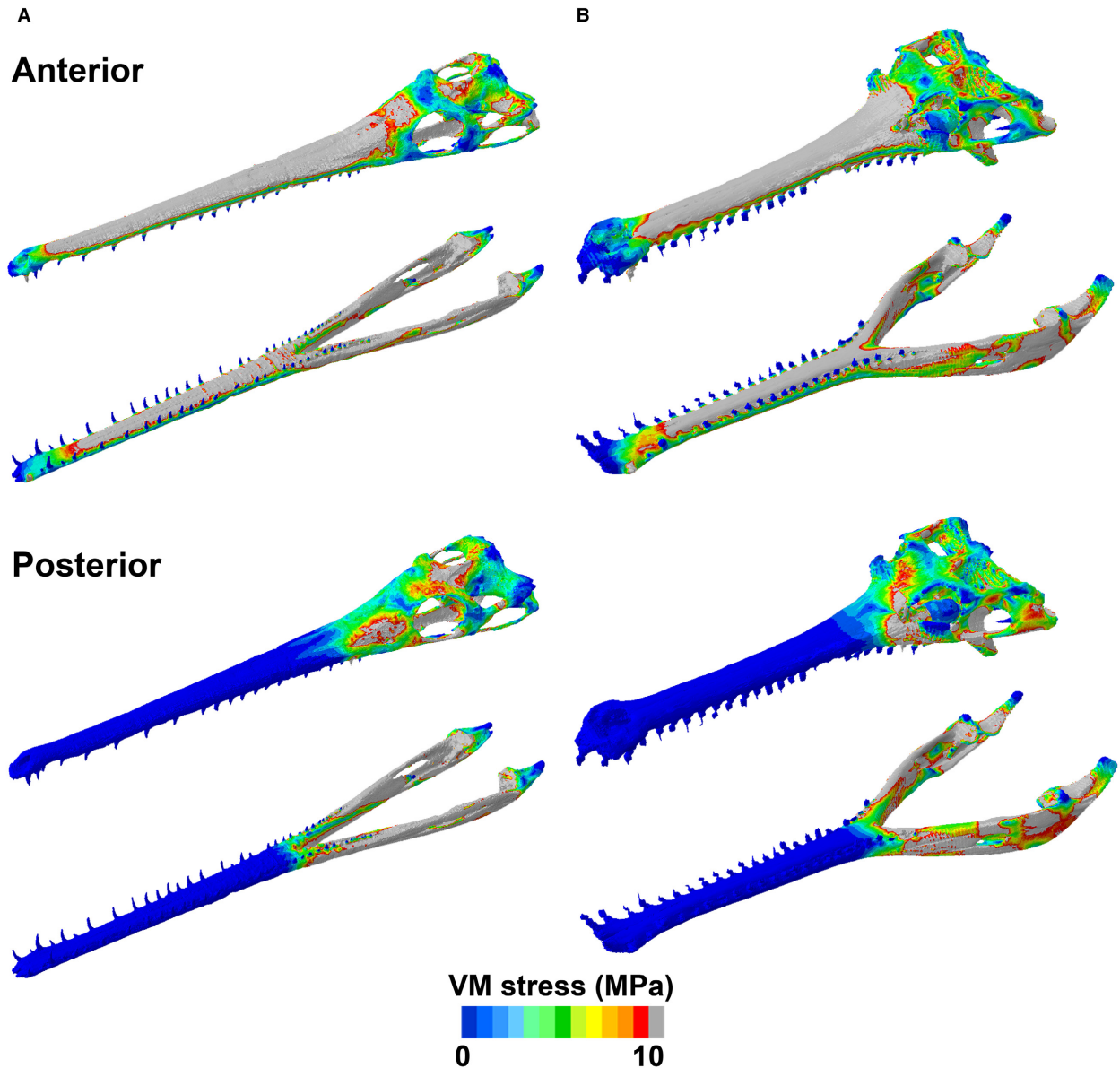
**FIG. 6.** Von Mises stress distribution plots of the skulls of *Pelagosaurus* (A) and *Gavialis* (B), simulating a unilateral biting scenario at the anterior and posterior tooth positions. Grey areas represent von Mises stress values higher than 10 MPa.

intermediate rates of evolution are baurusuchids (especially in the branch leading to *Campinasuchus*), the protosuchian *Protosuchus* and the basal crocodylomorphs *Terrestrisuchus* and *Pedeticosaurus*. Finally, significant shifts in rates of evolution, as indicated by a $\Delta_V/\Delta_B > 2$, are present in all branches within Thalattosuchia and Baurusuchidae, *Protosuchus* and *Terrestrisuchus*.

The clade that shows highest rates of evolution of MJD in all trees is Eusuchia (*Borealosuchus* + *Iharkutosuchus*), as well as its stem group, which includes *Bernissartia* and more derived taxa (Fig. 8; Ballell *et al.* 2019, figs S5, S7–S9, table S3). This group has diverse values of MJD, with

basal taxa exhibiting deeper jaws and more derived taxa possessing lower MJD, except for *Iharkutosuchus*. In accordance with the AMA results, rate acceleration occurs in *Protosuchus* and in the branch leading to Teleosauridae (a group with extremely low MJD values), although rates decrease in more exclusive lineages. For instance, the branch leading to *Pelagosaurus* is characterized by low evolutionary rates, although this taxon exhibits the lowest MJD of all thalattosuchians. Intermediate rates of evolution are seen in some basal crocodylomorphs (*Terrestrisuchus* and *Dibothrosuchus*), in the clade including *Stomatosuchus* and *Laganosuchus*, in the group uniting
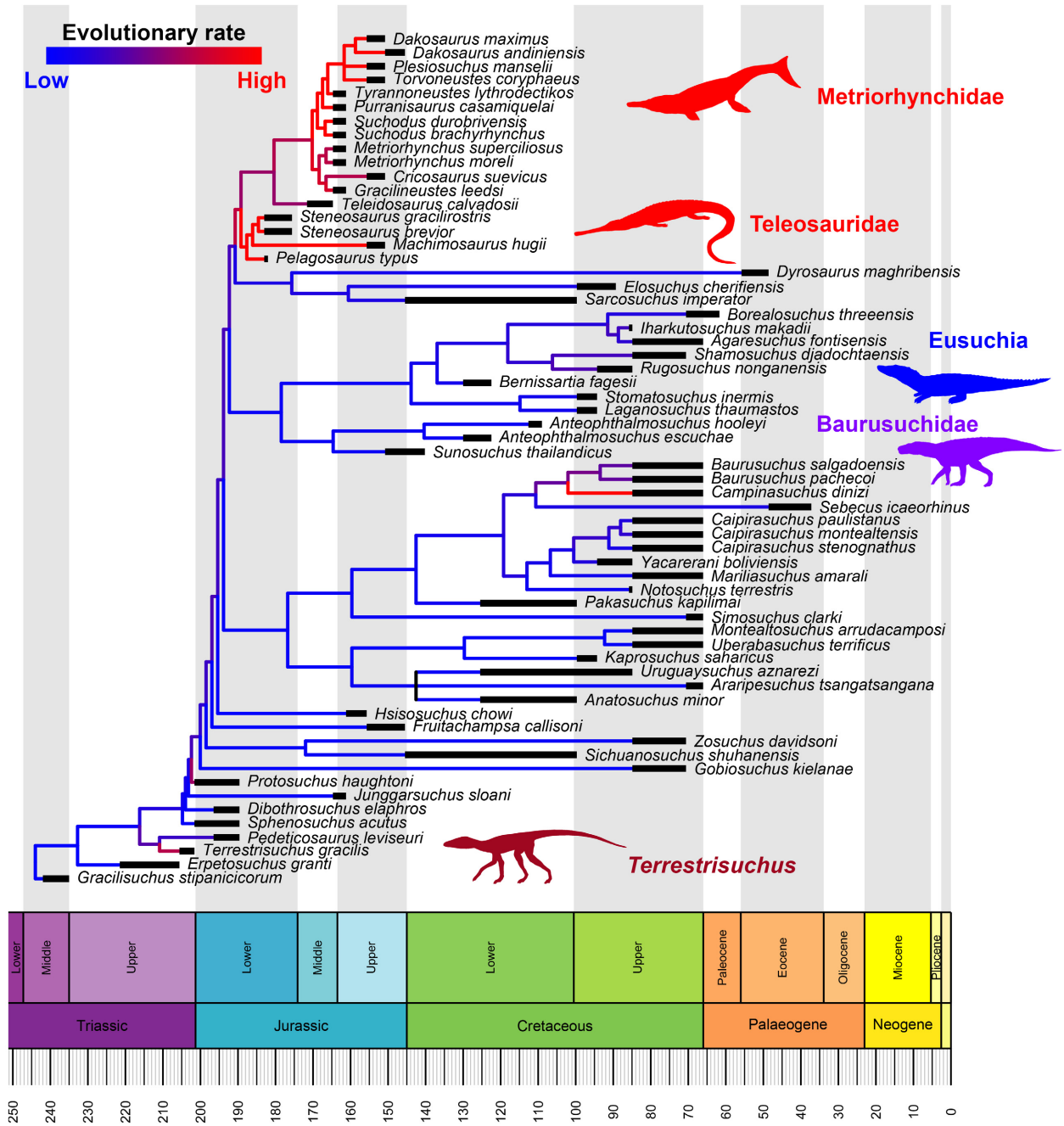
**FIG. 7.** Rates of evolution of anterior mechanical advantage (AMA) in Crocodylomorpha. Red branches indicate mean rate scalar values higher than 6 and blue branches, rate values close to 0. Purple branches represent intermediate evolutionary rates. Phylogenetic tree time-scaled using the equal branch length method.

pholidosaurs, dyrosaurs and thalattosuchians, and at the base of Thalattosuchia. Rate shifts in MJD are detected in the clade uniting *Bernissartia* and *Borealosuchus* and all the included branches, with the exception of the clade *Shamosuchus* + *Rugosuchus*. Coincident with the results for AMA, the branch leading to *Protosuchus* also experiences a significant shift in rates of evolution.

## DISCUSSION

*Functional convergence in* Pelagosaurus *and* Gavialis

Differences in muscle force production between mAME and mPT complexes are greater in *Gavialis*, reflecting the fact that its pterygoideus musculature is more developed.
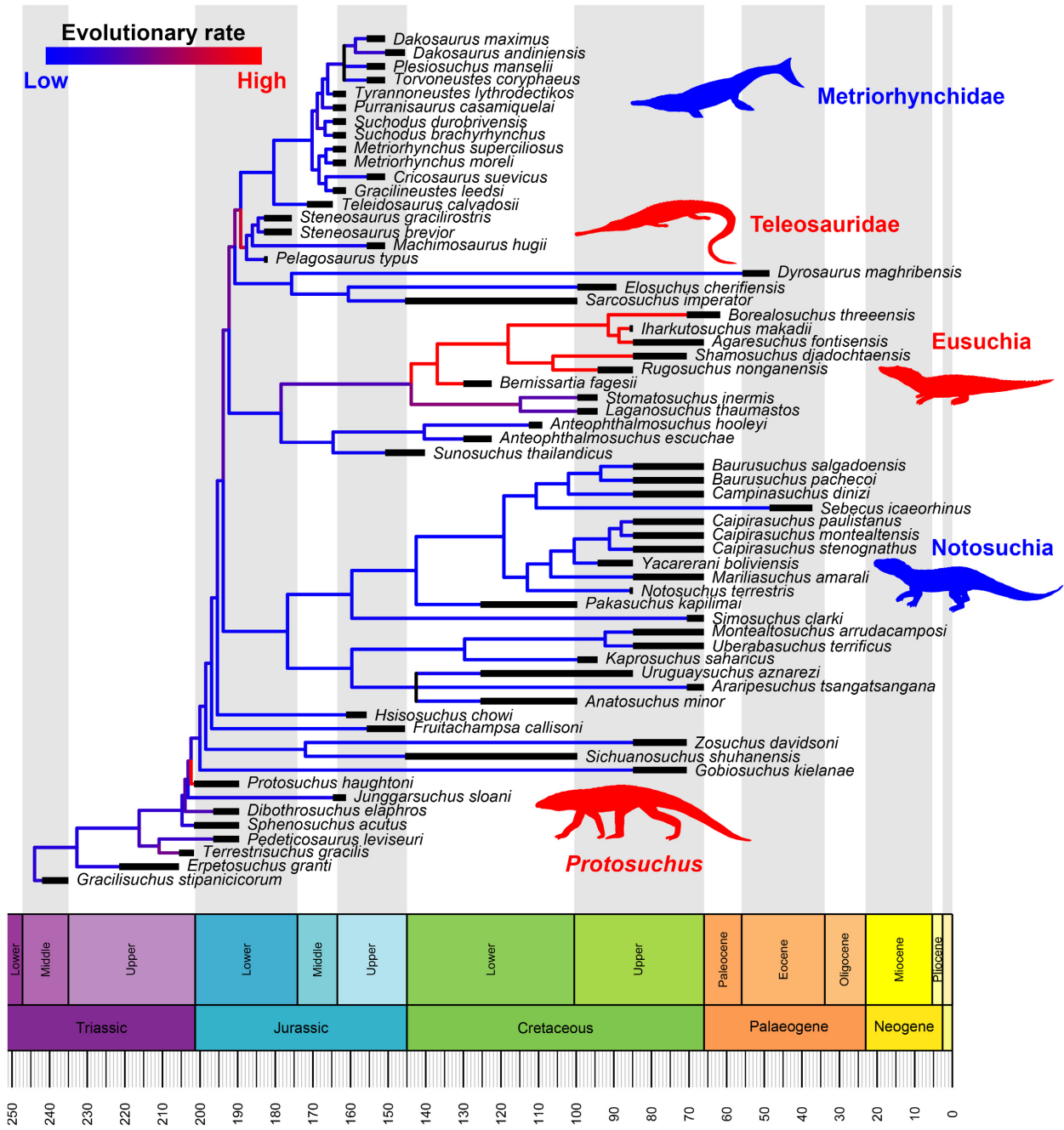
**FIG. 8.** Rates of evolution of size-corrected maximum jaw depth (MJD) in Crocodylomorpha. Red branches indicate mean rate scalar values higher than 4 and blue branches, rate values close to 0. Purple branches represent intermediate evolutionary rates. Phylogenetic tree time-scaled using the equal branch length method.

This was enabled by the elongation of the retroarticular process and the posteroventral growth of the pterygoid flanges, characteristic traits of derived eusuchians (Salisbury *et al.* 2006). The hypertrophied mPTv muscle is a distinctive character of extant crocodiles that has been linked to their ability to produce the most powerful bite forces known (Gignac & Erickson 2016). This muscle is extremely bulky and shows remarkable pennation, a condition that enables the concentration of a greater number of muscle fibres per unit area and therefore the generation of greater jaw-closing muscle forces (Gans *et al.* 1985; Gignac & Erickson 2016). In this sense, *Gavialis* differs from other crocodilians in having a relatively smaller mPTv that does not insert on the lateral surface of the retroarticular process (Endo *et al.* 2002). This autapomorphic arrangement of the jaw adductor musculature has a direct impact on

feeding, as the gharial was found to deviate from the rest of living crocodiles in its bite force, exerting the weakest bite among all members of the clade (Erickson *et al.* 2012). Despite this, the gharial possesses a bulkier mPT than *Pelagosaurus*, which has a short retroarticular process and unexpanded pterygoid flanges. Therefore, mAME must have been relatively more important in muscle force generation in thalattosuchians than in extant crocodiles, more closely resembling the jaw muscle arrangement of other archosaurs (Holliday & Witmer 2007).

Finite element models of *Gavialis* and *Pelagosaurus* responded in a similar but not identical fashion to feeding loads, suggesting potential differences in feeding mechanics and preferred prey. In both taxa, high stress is localized in the dorsal region of the snout and in the secondary palate, as expected for structures undergoing dorsoventral bending. The secondary palate is an apomorphic trait that evolved in crocodylomorphs and reached a fully formed condition in eusuchians (Salisbury *et al.* 2006). It has been demonstrated to confer biomechanical resistance to feeding loads in crocodilians (Busbey 1995; Rayfield *et al.* 2007). While this structure increases torsional resistance in platyrostral crocodiles, it is more effective for bending resistance in species with long, tubular snouts like the gharial (Rayfield *et al.* 2007) and by extension *Pelagosaurus*.

Bilateral bites cause stress in the dorsoventral direction (bending) while the torsional component of unilateral biting determines that stress acts in all directions (Dumont *et al.* 2005). Therefore, torsional loads cause an increase in stress at the sides of the snout in the unilateral biting scenario (Figs 5, 6). However, the patterns of stress distribution, especially at the back of the skull, and median stress magnitudes (Ballell *et al.* 2019, figs S1, S2) do not differ markedly between anterior bi and unilateral bite simulations. This is because even in unilateral biting the main direction of applied force is dorsoventral and applied muscle loads also generate stress in the posterior skull. Stress similarity may also be due to the short distances between tooth constraints on both sides of narrow, tubular snouts like those of *Pelagosaurus* and *Gavialis*. Differences in stress distribution between bilateral and unilateral loading are clearer in posterior bites as distances between constrained teeth are greater. However, stress magnitudes are similar in both scenarios, particularly in *Pelagosaurus* (Ballell *et al.* 2019, figs S1, S2).

The stress distribution in the skulls of the two study taxa matches FE models of other longirostrine extant crocodilians (McCurry *et al.* 2017*b*). High stress concentrates in the same anatomical regions, indicating that long-snouted crocodylomorphs accommodate feeding-induced stress in a similar fashion. The greater mechanical resistance of *Pelagosaurus* and *Gavalis* skulls at posterior bites compared to anterior bites (Fig. 5) also matches extant longirostrine crocodilians (McHenry *et al.* 2006),

which are able to better withstand relatively high bite forces comparable to those of brevirostrine taxa at caudal toothrow positions (McCurry *et al.* 2017*b*). This relation is reversed in other tetrapod groups such as some herbivorous dinosaurs, which experience higher cranial stresses when biting with their posterior teeth (Lautenschlager *et al.* 2016*b*). These results corroborate that the feeding mechanics of *Gavialis* resembles that of other longirostrine taxa in using the tip of the snout to catch prey with fast movements and the posterior teeth to produce higher bite forces that induce lower stress in the skull (Taylor 1987; McHenry *et al.* 2006). The similarities with *Pelagosaurus* suggest that the extinct species acquired this same feeding behaviour convergently.

If the effect of size is removed and skull shape is compared, the mandible of *Pelagosaurus* experiences greater feeding-induced stress than that of the gharial, although differences are not so evident when crania are compared (Ballell *et al.* 2019, figs S1, S2). Differences in skull morphology are responsible for this variation in performance, as the gharial has a more robust cranium that expands at the orbits, while that of the thalattosuchian is more gracile and dorsoventrally shorter. The mandible of *Pelagosaurus* is notably more slender and less deep than that of *Gavialis*, conferring less resistance to dorsoventral bending. So, in terms of mechanical resistance to higher feeding loads, it is the lower jaw of *Pelagosaurus* that suggests lower bite forces and softer prey. The evolution of dorsoventrally short and gracile mandibles was key in the origin of teleosaurids (Fig. 8, see below) and snout length was a determining factor of their diet, suggesting that these forms were highly specialized for piscivory and performing fast prey capture (Pierce *et al.* 2009). Additionally, comparative FE studies have interpreted higher stress within skulls as evidence for feeding on softer food items (Button *et al.* 2014) or on a more restricted diet (Lautenschlager *et al.* 2016*b*). Following this rationale, even though *Pelagosaurus* and *Gavialis* probably shared comparable feeding habits, the former seems to have been a more specialized piscivore that fed perhaps exclusively on soft, small, fast-moving prey. The study specimen represents a sub-adult whose jaw mechanics may have differed from the adult condition. The differences in size between the two original specimens might also influence the results, as the gharial is a large adult with a skull three times bigger than BRLSI M1413. Thus, mechanical dissimilarity not only reflects differences in ecology but also in ontogenetic state, and allometry likely accounts for part of the differences in jaw muscle force between the two species. However, BRLSI M1413 was not a very young animal so it is unlikely that it could have developed sufficient ontogenetic skull biomechanical modifications as an adult to offer the same biomechanical resistance as the gharial. Therefore, even though we may be inferring a juvenile diet, we infer this is also applicable to adult *Pelagosaurus*.

*Feeding and ecology of* Pelagosaurus

The morphological resemblance of their skulls has been suggested as evidence that the feeding ecology of *Pelagosaurus* was analogous to that of the gharial (Pierce & Benton 2006). *Gavialis gangeticus* is an endemic crocodilian from India that inhabits tropical fluvial environments of fast-flowing waters (Katdare *et al.* 2011). Although its diet is mainly fish, it opportunistically feeds on birds and mammals (Thorbjarnarson 1990). Adults can reach maximum recorded body sizes of six metres, making this species the second largest living crocodilian (Katdare *et al.* 2011) and the main piscivorous predator of Indian riverine ecosystems. Although other crocodilians inhabit Indian rivers, such as *Crocodylus palustris*, the gharial is the only crocodilian specialized for piscivory within this habitat, occupying a very specific ecological niche under low competitive pressures.

The palaeoenvironmental setting of *Pelagosaurus* differs from modern Indian rivers. In the Toarcian, Strawberry Bank (Somerset) was part of an epicontinental sea of shallow and warm waters in a tropical palaeolatitude similar to that of northern India (Pierce & Benton 2006). The fauna consisted of insects flying overhead, and nektonic ammonites, teuthid cephalopods and diverse actinopterygian fishes, including the large and thick-scaled *Pachycormus* and the small *Leptolepis* (Williams *et al.* 2015). Other tetrapods discovered at Strawberry Bank are juveniles of two species of ichthyosaur, *Stenopterygius triscissus* and *Hauffiopteryx typicus* (Caine & Benton 2011; Williams *et al.* 2015). While *Stenopterygius* possessed more robust and blunt teeth suggesting placement in Massare's (1987) 'smash' guild, *Hauffiopteryx* had long, piercing teeth, similar to *Pelagosaurus*, suggesting a mainly piscivorous diet (Caine & Benton 2011).

*Pelagosaurus*, unlike the semiaquatic gharial, was fully marine and only ventured on land to lay eggs (Pierce & Benton 2006). The lifestyle of this species is supported by its derived physiological, neuroanatomical and sensory adaptations, such as pyramidal semicircular canals, an elongated cochlear duct and possibly nasal salt glands (Pierce *et al.* 2017). Pierce *et al.* (2009) classified *Pelagosaurus* within the 'pierce I' guild of Massare (1987), a very specialized feeding guild with a diet consisting of small fish and soft-bodied cephalopods. Both kinds of prey were present in the palaeoenvironment that *Pelagosaurus* inhabited, and direct evidence of this species feeding on small *Leptolepis* is provided by gut contents (Pierce & Benton 2006). Our FE results support this, suggesting that the lower mechanical resistance of *Pelagosaurus* is related to the intake of small and soft food items, even though prey capture was probably achieved by lateral head sweeps, as in the gharial. In contrast, the more powerful jaw muscles and higher mechanical resistance of the skull of *Gavialis*, as well as its greater body size, enables it to feed on large fish and occasionally on larger and tougher prey such as tetrapods. These findings support the classic view that *Pelagosaurus* and other teleosaurs were adapted to catching fast-moving prey, just like extant longirostrine species (Massare 1987; Hua & de Buffrenil 1996) and shows that they might have been even more specialized than modern forms. The competitive pressures from sharing the same marine habitat with other piscivorous marine reptiles such as ichthyosaurs might be responsible for the highly specialized diet of *Pelagosaurus,* representing a case of niche partitioning in the marine reptile faunas of the Toarcian.

*Evolution of feeding modes in Crocodylomorpha*

The tempo of evolution of functional characters of the mandible sheds light on the evolutionary and ecological dynamics of crocodylomorphs. High rates of evolution of feeding-related traits are expected in clades that occupy empty adaptive zones and evolve novel feeding strategies in new environmental settings. Thalattosuchians were the first lineage of crocodylomorphs that invaded the marine realm and adapted to new kinds of diet and prey capture mechanisms (Pierce *et al.* 2009; Young *et al.* 2010). The rates analysis shows that the modification of jaw mechanics by anterior mechanical advantage (AMA) reduction was relevant in the functional evolution and radiation of this group (Fig. 7). Low AMA is linked to the evolution of longirostry in this group, as long snouts have a longer distance from the biting point to the jaw joint (outlevers), thus reducing the efficiency of transforming muscle force into bite force. However, a low mechanical advantage also involves greater speed of jaw closure, which may be important for catching agile prey (e.g. fish, cephalopods). The variability in this character among thalattosuchians, especially in metriorhynchids (Ballell *et al.* 2019, table S2), suggests that different lineages evolved mandibles able to generate either powerful or fast bites, determining their dietary preferences, with hypercarnivores such as *Dakosaurus* (Young *et al.* 2012*b*) and piscivores such as *Cricosaurus* (Young *et al.* 2010) at the two ends of the spectrum. The low AMA of *Pelagosaurus* results from a very elongated mandible and a mAME insertion positioned close to the jaw joint. The fast evolution of this trait in *Pelagosaurus* agrees with the FEA results and supports the idea that this species comprised specialists that relied on snapping bites to catch agile and soft prey. Therefore, continuous accelerated rates of evolution of this trait relate to the origin of divergent feeding modes among thalattosuchians. However, this functional innovation was not correlated with an increase in morphological disparity, probably due to the hydrodynamic

constraints imposed on skull shape by the aquatic environment (Stubbs *et al.* 2013), conserving a streamlined head profile to move efficiently in water (McHenry *et al.* 2006).

Rate acceleration in size-corrected maximum jaw depth (MJD) at the base of Teleosauridae (Fig. 8) supports a rapid radiation of this group within a specific adaptive zone. When the clade originated, they evolved extremely elongated and dorsoventrally short mandibles with long mandibular symphyses. Teleosaurids were mostly piscivorous forms specialized to catch prey by lateral head movements (Pierce *et al.* 2009). This kind of feeding mode does not entail great bending stress acting on the jaws during feeding. The high feeding-induced stresses registered in the long and dorsoventrally low mandible of *Pelagosaurus*, a condition which might be applicable to other teleosaurids, reflect this loading regime and are indicative of a specialized feeding adaptation. Therefore, rapid acquisition of gracile mandibles in teleosaurids was a result of positive selection towards their characteristic feeding behaviour, shared with longirostrine metriorhynchids (Pierce *et al.* 2009).

The differences in evolutionary rates between the two thalattosuchian clades may reflect divergent mechanisms of feeding evolution. Teleosaurids maintained higher evolutionary rates, indicating a rapid radiation of this more basal lineage during the Early Jurassic, filling empty ecospace in a less competitive environment after the end-Triassic mass extinction, which caused a drastic loss of diversity and disparity of marine reptiles (Thorne *et al.* 2011; Stubbs & Benton 2016). In contrast the pace of functional evolution was slower in metrorhynchids, which nonetheless exhibited a greater diversity of diets and feeding modes than teleosaurids, as indicated by their wider range of craniodental morphologies and skull biomechanical variability (Pierce *et al.* 2009; Young *et al.* 2010). In the Middle and Late Jurassic, the greatest ecomorphological diversification of marine reptiles during thalattosuchian existence took place (Stubbs & Benton 2016). During this time ecological niches in the marine realm may have been saturated, leading to intense competitive pressure among thalattosuchians (Young *et al.* 2010) and with other contemporary marine reptiles (Stubbs & Benton 2016). Pliosaurs achieved their highest dental disparity in the Late Jurassic suggesting diverse feeding strategies (Zverkov *et al.* 2018), some of them being marine apex predators (Foffa *et al.* 2014) as geosaurine metriorhynchids were (Young *et al.* 2010, 2012*a*, *b*). Feeding competition could have occurred with other contemporary marine reptiles such as ichthyosaurs and turtles (Stubbs & Benton 2016). Therefore, other evolutionary mechanisms such as niche partitioning, which has been documented in metriorhynchids (Young *et al.* 2010, 2012*b*) (and more generally among marine reptiles; Foffa *et al.* 2018) may have had more relevance in the feeding diversification of this group, which occurred at a slower tempo.

Evolutionary rates of the two selected functional characters yield surprising results for Notosuchia. This clade of mesoeucrocodylians inhabited Gondwana during the Cretaceous (Carvalho *et al.* 2010), evolved an outstanding diversity of feeding modes and filled multiple ecological niches (Stubbs *et al.* 2013), some of them occupied by mammals in other parts of the globe (O'Connor *et al.* 2010). Their feeding ecologies ranged from highly specialized carnivory in the Baurusuchidae (Nascimento & Zaher 2011; Godoy *et al.* 2018) to herbivory with heterodont dentitions and complex jaw movements (Nobre *et al.* 2008; O'Connor *et al.* 2010). This functional richness was responsible for the rise of notosuchians as the main radiation of crocodylomorphs during the Cretaceous (Stubbs *et al.* 2013; Bronzati *et al.* 2015). Therefore, the low rates of evolution of AMA and MJD observed in this clade seem to contradict the idea that notosuchians radiated into new niches in the Cretaceous. Only baurusuchids show moderately high rates of MJD, which may indicate that changes in mandibular depth and thus resistance to dorsoventral bending was an important factor in the evolution of this family. However, in other notosuchians, feeding innovation could have arisen by morphofunctional changes in other parts of the skull and even in the postcranial skeleton (Stubbs *et al.* 2013). For instance, their very complex and diverse dentitions could have played a more important role than functional changes in the mandible for the feeding diversification of the clade.

Eusuchians represent the second radiation of crocodylomorphs during the Cretaceous (Bronzati *et al.* 2015). The MJD rate acceleration detected in this clade (Fig. 8) is consistent with their diversification in the Early Cretaceous and their conquest of a new adaptive zone (Martin & Delfino 2010). Eusuchians show a trend towards jaw depth reduction and elongation of the mandible (Ballell *et al.* 2019, table S2), that led to the evolution of longirostrine skulls seen in extant crocodiles. The family Hylaeochampsidae, including *Iharkutosuchus* (Ösi *et al.* 2007), is an exception to this trend, as they possessed robust and brevirostrine skulls with deep jaws. The elongation and dorsoventral shortening of the mandible also had an adaptive relevance not directly related to feeding. This trait is linked to the evolution of platyrostral skulls, important in the conquest of the semiaquatic ambush predator niche by eusuchians (Salisbury *et al.* 2006), as it enabled them to maintain a low profile in water. Eusuchia and particularly Crocodylia were highly specialized forms that acquired unique feeding behaviours such as the 'death roll', which was enabled by the increased torsional resistance provided by the autapomorphic full secondary palate (Salisbury *et al.* 2006; Rayfield *et al.* 2007).

## CONCLUSIONS

In this study we tested the proposed functional convergence between *Pelagosaurus* and *Gavialis*. Digital muscle reconstruction and FE modelling confirm that *Pelagosaurus* shares a similar biomechanical behaviour with *Gavialis* as a consequence of longirostry. However, the higher stresses recorded in the skull of *Pelagosaurus* suggest that the two taxa occupied slightly different ecological niches. Instead, our results suggest that the thalattosuchian was a particularly specialized piscivore that fed on softer and smaller prey than the gharial. Palaeoenvironmental conditions and ecological interactions with other marine reptiles may have played a role in the acquisition of this particular feeding strategy. Consequently, this study notes the limitations of relying only on morphological similarity when testing functional hypotheses in fossils and supports previous work that highlights the relevance of testing functional convergence with extant models to infer feeding habits in extinct taxa.

Patterns of evolutionary rates indicate that functional innovation in the mandible was an important factor in the radiation of some crocodylomorph clades by allowing development of novel feeding strategies. Constant evolutionary changes in AMA were a driving force for feeding specialization within Thalattosuchia, while MJD evolutionary rates support an 'early burst' of evolution at the origin of teleosaurids, associated with the acquisition of a new feeding strategy. Dissimilar rates of evolution between the two thalattosuchian clades suggest that in the Early Jurassic, teleosaurids rapidly radiated into an empty ecological niche, while metriorhynchids diversified more slowly in the more competitive Late Jurassic marine environment. Finally, decrease in jaw depth was a mechanism that facilitated the ecological transition of eusuchians to become semiaquatic ambush predators.

## DATA ARCHIVING STATEMENT

## REFERENCES

ANDERSON, P. S. L. 2009. Biomechanics, functional patterns, and disparity in Late Devonian arthrodires. *Paleobiology*, **35**, 321–342.

—— FRIEDMAN, M. and RUTA, M. 2013. Late to the table: diversification of tetrapod mandibular biomechanics lagged behind the evolution of terrestriality. *Integrative & Comparative Biology*, **53**, 197–208.

BAKER, J., MEADE, A., PAGEL, M. and VENDITTI, C. 2016. Positive phenotypic selection inferred from phylogenies. *Biological Journal of the Linnean Society*, **118**, 95–115.

BALLELL, A., MOON, B. C., PORRO, L. B., BENTON, M. J. and RAYFIELD, E. J. 2019. Data from: Convergence and functional evolution of longirostry in crocodylomorphs. *Dryad Digital Repository*. https://doi.org/10.5061/dryad.b3s4v0g

BAPST, D. W. 2012. paleotree: an R package for paleontological and phylogenetic analyses of evolution. *Methods in Ecology & Evolution*, **3**, 803–807.

BATES, K. T. and FALKINGHAM, P. L. 2012. Estimating maximum bite performance in *Tyrannosaurus rex* using multibody dynamics. *Biology Letters*, **8**, 660–664.

—— —— 2018. The importance of muscle architecture in biomechanical reconstructions of extinct animals: a case study using *Tyrannosaurus rex*. *Journal of Anatomy*, **233**, 625–635.

BELL, M. A. and LLOYD, G. T. 2015. strap: an R package for plotting phylogenies against stratigraphy and assessing their stratigraphic congruence. *Palaeontology*, **58**, 379–389.

BENTON, M. J. and WALKER, A. D. 2002. *Erpetosuchus*, a crocodile-like basal archosaur from the Late Triassic of Elgin, Scotland. *Zoological Journal of the Linnean Society*, **136**, 25–47.

BRIGHT, J. A. and RAYFIELD, E. J. 2011. The response of cranial biomechanical finite element models to variations in mesh density. *Anatomical Record*, **294**, 610–620.

BRONZATI, M., MONTEFELTRO, F. C. and LANGER, M. C. 2012. A species-level supertree of Crocodyliformes. *Historical Biology*, **24**, 598–606.

—— —— —— 2015. Diversification events and the effects of mass extinctions on Crocodyliformes evolutionary history. *Royal Society Open Science* **2**, 140385.

BRUSATTE, S. L., BENTON, M. J., RUTA, M. and LLOYD, G. T. 2008. The first 50 Myr of dinosaur evolution: macroevolutionary pattern and morphological disparity. *Biology Letters*, **4**, 733–736.

—— —— DESOJO, J. B. and LANGER, M. C. 2010. The higher-level phylogeny of Archosauria (Tetrapoda: Diapsida). *Journal of Systematic Palaeontology*, **8**, 3–47.

BUSBEY, A. B. III. 1995. The structural consequences of skull flattening in crocodilians. 173–192. *In* THOMASON, J. J.

(ed.) *Functional morphology in vertebrate paleontology*. Cambridge University Press.

BUSCALIONI, A. D. 2017. The Gobiosuchidae in the early evolution of Crocodyliformes. *Journal of Vertebrate Paleontology*, **37**, e1324459.

BUTLER, R. J., SULLIVAN, C., EZCURRA, M. D., LIU, J., LECUONA, A. and SOOKIAS, R. B. 2014. New clade of enigmatic early archosaurs yields insights into early pseudosuchian phylogeny and the biogeography of the archosaur radiation. *BMC Evolutionary Biology*, **14**, 128.

BUTTON, D. J., RAYFIELD, E. J. and BARRETT, P. M. 2014. Cranial biomechanics underpins high sauropod diversity in resource-poor environments. *Proceedings of the Royal Society B*, **281**, 20142114.

—— BARRETT, P. M. and RAYFIELD, E. J. 2016. Comparative cranial myology and biomechanics of *Plateosaurus* and *Camarasaurus* and evolution of the sauropod feeding apparatus. *Palaeontology*, **59**, 887–913.

—— —— —— 2017. Craniodental functional evolution in sauropodomorph dinosaurs. *Paleobiology* **43**, 435–462.

CAINE, H. and BENTON, M. J. 2011. Ichthyosauria from the Upper Lias of Strawberry Bank, England. *Palaeontology*, **54**, 1069–1093.

CARVALHO, I. D., GASPARINI, Z. B., SALGADO, L., VASCONCELLOS, F. M. and MARINHO, T. D. 2010. Climate's role in the distribution of the Cretaceous terrestrial Crocodyliformes throughout Gondwana. *Palaeogeography Palaeoclimatology Palaeoecology*, **297**, 252–262.

CLARK, J. M., XU, X., FORSTER, C. A. and WANG, Y. 2004. A Middle Jurassic 'sphenosuchian' from China and the origin of the crocodylian skull. *Nature*, **430**, 1021–1024.

CUFF, A. R. and RAYFIELD, E. J. 2013. Feeding mechanics in spinosaurid theropods and extant crocodilians. *PLoS One*, **8**, e65295.

DUMONT, E. R., PICCIRILLO, J. and GROSSE, L. R. 2005. Finite-element analysis of biting behavior and bone stress in the facial skeletons of bats. *Anatomical Record Part A*, **283A**, 319–330.

—— GROSSE, I. R. and SLATER, G. J. 2009. Requirements for comparing the performance of finite element models of biological structures. *Journal of Theoretical Biology*, **256**, 96–103.

ENDO, H., AOKI, R., TARU, H., KIMURA, J., SASAKI, M., YAMAMOTO, M., ARISHIMA, K. and HAYASHI, Y. 2002. Comparative functional morphology of the masticatory apparatus in the long-snouted crocodiles. *Anatomia Histologia Embryologia-Journal of Veterinary Medicine Series C*, **31**, 206–213.

ERICKSON, G. M., GIGNAC, P. M., STEPPAN, S. J., LAPPIN, A. K., VLIET, K. A., BRUEGGEN, J. D., INOUYE, B. D., KLEDZIK, D. and WEBB, G. J. W. 2012. Insights into the ecology and evolutionary euccess of crocodilians revealed through bite-force and tooth-pressure experimentation. *PLoS One*, **7**, e31781.

ERWIN, D. H. 1992. A preliminary classification of evolutionary radiations. *Historical Biology*, **6**, 133–147.

FOFFA, D., CUFF, A. R., SASSOON, J., RAYFIELD, E. J., MAVROGORDATO, M. N. and BENTON, M. J. 2014. Functional anatomy and feeding biomechanics of a giant Upper Jurassic pliosaur (Reptilia: Sauropterygia) from Weymouth Bay, Dorset, UK. *Journal of Anatomy*, **225**, 209–219.

—— YOUNG, M. T., STUBBS, T. L., DEXTER, K. G. and BRUSATTE, S. L. 2018. The long-term ecology and evolution of marine reptiles in a Jurassic seaway. *Nature Ecology & Evolution*, **2**, 1548–1555.

FOOTE, M. 1994. Morphological disparity in Ordovician-Devonian crinoids and the early saturation of morphological space. *Paleobiology*, **20**, 320–344.

GANS, C., DEVREE, F. and CARRIER, D. 1985. Usage pattern of the complex masticatory muscles in the shingleback lizard, *Trachydosaurus rugosus*: a model for muscle placement. *American Journal of Anatomy*, **173**, 219–240.

GIGNAC, P. M. and ERICKSON, G. M. 2016. Ontogenetic bite-force modeling of *Alligator mississippiensis*: implications for dietary transitions in a large-bodied vertebrate and the evolution of crocodylian feeding. *Journal of Zoology*, **299**, 229–238.

GILL, P. G., PURNELL, M. A., CRUMPTON, N., BROWN, K. R., GOSTLING, N. J., STAMPANONI, M. and RAYFIELD, E. J. 2014. Dietary specializations and diversity in feeding ecology of the earliest stem mammals. *Nature*, **512**, 303–305.

GODOY, P. L., FERREIRA, G. S., MONTEFELTRO, F. C., NOVA, B. C. V., BUTLER, R. J. and LANGER, M. C. 2018. Evidence for heterochrony in the cranial evolution of fossil crocodyliforms. *Palaeontology*, **61**, 543–558.

HEATH, T. A., HUELSENBECK, J. P. and STADLER, T. 2014. The fossilized birth–death process for coherent calibration of divergence-time estimates. *Proceedings of the National Academy of Sciences*, **111**, E2957–E2966.

HOLLIDAY, C. M. and WITMER, L. M. 2007. Archosaur adductor chamber evolution: integration of musculoskeletal and topological criteria in jaw muscle homology. *Journal of Morphology*, **268**, 457–484.

—— TSAI, H. P., SKILJAN, R. J., GEORGE, I. D. and PATHAN, S. 2013. A 3D interactive model and atlas of the jaw musculature of *Alligator mississippiensis*. *PLoS One*, **8**, e62806.

HUA, S. and BUFFRENIL, V. DE 1996. Bone histology as a clue in the interpretation of functional adaptations in the Thalattosuchia (Reptilia, Crocodylia). *Journal of Vertebrate Paleontology*, **16**, 703–717.

IORDANSKY, N. 1964. The jaw muscles of the crocodiles and some relating structures of the crocodilian skull. *Anatomischer Anzeiger*, **115**, 256–280.

—— 2011. Jaw muscles of the crocodiles: structure, synonymy, and some implications on homology and functions. *Russian Journal of Herpetology*, **7**, 41–50.

IRMIS, R. B., NESBITT, S. J. and SUES, H. D. 2013. Early Crocodylomorpha. 275–302. *In* NESBIT, T. S. J., DESOJO, J. B. and IRMIS, R. B. (eds). *Anatomy, phylogeny and palaeobiology of early archosaurs and their kin*. Geological Society, London, Special Publications, **379**, 608 pp.

JONES, M. E. H. 2008. Skull shape and feeding strategy in *Sphenodon* and other Rhynchocephalia (Diapsida: Lepidosauria). *Journal of Morphology*, **269**, 945–966.

KATDARE, S., SRIVATHSA, A., JOSHI, A., PANKE, P., PANDE, R., KHANDAL, D. and EVERARD, M. 2011.

Gharial (*Gavialis gangeticus*) populations and human influences on habitat on the River Chambal, India. *Aquatic Conservation: Marine & Freshwater Ecosystems*, **21**, 364–371.

KELLNER, A. W. A., PINHEIRO, A. E. P. and CAMPOS, D. A. 2014. A new sebecid from the Paleogene of Brazil and the crocodyliform radiation after the K–Pg boundary. *PLoS One*, **9**, e81386.

LAURIN, M. 2004. The evolution of body size, Cope's rule and the origin of amniotes. *Systematic Biology*, **53**, 594–622.

LAUTENSCHLAGER, S. 2013. Cranial myology and bite force performance of *Erlikosaurus andrewsi*: a novel approach for digital muscle reconstructions. *Journal of Anatomy*, **222**, 260–272.

—— 2016. Reconstructing the past: methods and techniques for the digital restoration of fossils. *Royal Society Open Science*, **3**, 160342.

—— WITZMANN, F. and WERNEBURG, I. 2016a. Palate anatomy and morphofunctional aspects of interpterygoid vacuities in temnospondyl cranial evolution. *Science of Nature*, **103**, 79.

—— BRASSEY, C. A., BUTTON, D. J. and BARRETT, P. M. 2016b. Decoupled form and function in disparate herbivorous dinosaur clades. *Scientific Reports*, **6**, 26495.

LEARDI, J. M., POL, D., NOVAS, F. E. and RIGLOS, M. S. 2015. The postcranial anatomy of Y*acarerani boliviensis* and the phylogenetic significance of the notosuchian postcranial skeleton. *Journal of Vertebrate Paleontology*, **35**, e995187.

LEE, M. S. Y. and YATES, A. M. 2018. Tip-dating and homoplasy: reconciling the shallow molecular divergences of modern gharials with their long fossil record. *Proceedings of the Royal Society B*, **285**, 20181071.

LEMON, J. 2006. plotrix: a package in the red light district of R. *R-News*, **6**, 8–12.

LLOYD, G. T., WANG, S. C. and BRUSATTE, S. L. 2012. Identifying heterogeneity in rates of morphological evolution: discrete character change in the evolution of lungfish (Sarcopterygii; Dipnoi). *Evolution*, **66**, 330–348.

MACLAREN, J. A., ANDERSON, P. S. L., BARRETT, P. M. and RAYFIELD, E. J. 2017. Herbivorous dinosaur jaw disparity and its relationship to extrinsic evolutionary drivers. *Paleobiology*, **43**, 15–33.

MALLON, J. C. and ANDERSON, J. S. 2015. Jaw mechanics and evolutionary paleoecology of the megaherbivorous dinosaurs from the Dinosaur Park Formation (upper Campanian) of Alberta, Canada. *Journal of Vertebrate Paleontology*, **35**, e904323.

MARTIN, J. E. and DELFINO, M. 2010. Recent advances in the comprehension of the biogeography of Cretaceous European eusuchians. *Palaeogeography, Palaeoclimatology, Palaeoecology*, **293**, 406–418.

MASSARE, J. A. 1987. Tooth morphology and prey preference of Mesozoic marine reptiles. *Journal of Vertebrate Paleontology*, **7**, 121–137.

MATZKE, N. J. and WRIGHT, A. M. 2016. Inferring node dates from tip dates in fossil Canidae: the importance of tree priors. *Biology Letters*, **12**, 20160328.

MCCURRY, M. R., EVANS, A. R., FITZGERALD, E. M. G., ADAMS, J. W., CLAUSEN, P. D. and McHENRY, C. R. 2017a. The remarkable convergence of skull shape in crocodilians and toothed whales. *Proceedings of the Royal Society B*, **284**, 20162348.

—— WALMSLEY, C. W., FITZGERALD, E. M. G. and McHENRY, C. R. 2017b. The biomechanical consequences of longirostry in crocodilians and odontocetes. *Journal of Biomechanics*, **56**, 61–70.

McHENRY, C. R., CLAUSEN, P. D., DANIEL, W. J. T., MEERS, M. B. and PENDHARKAR, A. 2006. Biomechanics of the rostrum in crocodilians: a comparative analysis using finite-element modeling. *Anatomical Record Part A*, **288A**, 827–849.

MUELLER-TÖWE, I. J. 2006. Anatomy, phylogeny, and palaeoecology of the basal thalattosuchians (Mesoeucrocodylia) from the Liassic of Central Europe. Unpublished PhD thesis, Universität Mainz, Germany, 369 pp.

NASCIMENTO, P. M. and ZAHER, H. 2011. The skull of the Upper Cretaceous baurusuchid crocodile *Baurusuchus albertoi* Nascimento & Zaher 2010, and its phylogenetic affinities. *Zoological Journal of the Linnean Society*, **163**, S116–S131.

NEENAN, J. M., RUTA, M., CLACK, J. A. and RAYFIELD, E. J. 2014. Feeding biomechanics in *Acanthostega* and across the fish - tetrapod transition. *Proceedings of the Royal Society B*, **281**, 20132689.

NOBRE, P. H., CARVALHO, I. D., DE VASCONCELLOS, F. M. and SOUTO, P. R. 2008. Feeding behavior of the gondwanic Crocodylomorpha *Mariliasuchus amarali* from the Upper Cretaceous Bauru Basin, Brazil. *Gondwana Research*, **13**, 139–145.

O'CONNOR, P. M., SERTICH, J. J. W., STEVENS, N. J., ROBERTS, E. M., GOTTFRIED, M. D., HIERONYMUS, T. L., JINNAH, Z. A., RIDGELY, R., NGASALA, S. E. and TEMBA, J. 2010. The evolution of mammal-like crocodyliforms in the Cretaceous Period of Gondwana. *Nature*, **466**, 748–751.

ÖSI, A., CLARK, J. M. and WEISHAMPEL, D. B. 2007. First report on a new basal eusuchian crocodyliform with multicusped teeth from the Upper Cretaceous (Santonian) of Hungary. *Neues Jahrbuch für Geologie und Paläontologie, Abhandlungen*, **243**, 169–177.

PARADIS, E., CLAUDE, J. and STRIMMER, K. 2004. ape: analyses of phylogenetics and evolution in R language. *Bioinformatics*, **20**, 289–290.

PIERCE, S. E. and BENTON, M. J. 2006. *Pelagosaurus typus* Bronn, 1841 (Mesoeucrocodylia: Thalattosuchia) from the Upper Lias (Toarcian, Lower Jurassic) of Somerset, England. *Journal of Vertebrate Paleontology*, **26**, 621–635.

—— ANGIELCZYK, K. D. and RAYFIELD, E. J. 2009. Shape and mechanics in thalattosuchian (Crocodylomorpha) skulls: implications for feeding behaviour and niche partitioning. *Journal of Anatomy*, **215**, 555–576.

—— WILLIAMS, M. and BENSON, R. B. J. 2017. Virtual reconstruction of the endocranial anatomy of the early Jurassic marine crocodylomorph *Pelagosaurus typus* (Thalattosuchia). *PeerJ*, **5**, e3225.

POL, D., NASCIMENTO, P. M., CARVALHO, A. B., RICCOMINI, C., PIRES-DOMINGUES, R. A. and ZAHER, H. 2014. A new notosuchian from the Late Cretaceous of Brazil and the phylogeny of advanced notosuchians. *PLoS One*, **9**, e93105.

PORRO, L. B., HOLLIDAY, C. M., ANAPOL, F., ONTI-VEROS, L. C., ONTIVEROS, L. T. and ROSS, C. F. 2011. Free body analysis, beam mechanics, and finite element modeling of the mandible of *Alligator mississippiensis*. *Journal of Morphology*, **272**, 910–937.

R CORE TEAM. 2017. R: a language and environment for statistical computing. v3.4.2. R Foundation for Statistical Computing. https://www.R-project.org

RAYFIELD, E. J. 2004. Cranial mechanics and feeding in *Tyrannosaurus rex*. *Proceedings of the Royal Society B*, **271**, 1451–1459.

—— 2007. Finite element analysis and understanding the biomechanics and evolution of living and fossil organisms. *Annual Review of Earth & Planetary Sciences*, **35**, 541–576.

—— MILNER, A. C., XUAN, V. B. and YOUNG, P. G. 2007. Functional morphology of spinosaur 'crocodile-mimic' dinosaurs. *Journal of Vertebrate Paleontology*, **27**, 892–901.

RONQUIST, R., TESLENKO, M., MARK, P. VAN DER, AYRES, D. L., DARLING, A., HÖHNA, S., LARGET, B., LIU, L., SUCHARD, M. A. and HUELSENBECK, J. P. 2012. MrBayes 3.2: efficient Bayesian phylogenetic inference and model choice across a large model space. *Systematic Biology*, **61**, 539–542.

SALISBURY, S. W., MOLNAR, R. E., FREY, E. and WILLIS, P. M. A. 2006. The origin of modern crocodyliforms: new evidence from the Cretaceous of Australia. *Proceedings of the Royal Society B*, **273**, 2439–2448.

SCHNEIDER, C. A., RASBAND, W. S. and ELICEIRI, K. W. 2012. NIH Image to ImageJ: 25 years of image analysis. *Nature Methods*, **9**, 671–675.

SELLERS, K. C., MIDDLETON, K. M., DAVIS, J. L. and HOLLIDAY, C. M. 2017. Ontogeny of bite force in a validated biomechanical model of the American alligator. *Journal of Experimental Biology*, **220**, 2036–2046.

STUBBS, T. L. and BENTON, M. J. 2016. Ecomorphological diversifications of Mesozoic marine reptiles: the roles of ecological opportunity and extinction. *Paleobiology*, **42**, 547–573.

—— PIERCE, S. E., RAYFIELD, E. J. and ANDERSON, P. S. L. 2013. Morphological and biomechanical disparity of crocodile-line archosaurs following the end-Triassic extinction. *Proceedings of the Royal Society B*, **280**, 20131940.

TAYLOR, M. A. 1987. How tetrapods feed in water: a functional analysis by paradigm. *Zoological Journal of the Linnean Society*, **91**, 171–195.

TAYLOR, A. C., LAUTENSCHLAGER, S., QI, Z. and RAYFIELD, E. J. 2017. Biomechanical evaluation of different musculoskeletal arrangements in *Psittacosaurus* and implications for cranial function. *Anatomical Record*, **300**, 49–61.

THOMASON, J. J. 1991. Cranial strength in relation to estimated biting forces in some mammals. *Canadian Journal of Zoology*, **69**, 2326–2333.

THORBJARNARSON, J. B. 1990. Notes on the feeding behavior of the gharial (*Gavialis gangeticus*) under seminatural conditions. *Journal of Herpetology*, **24**, 99–100.

THORNE, P. M., RUTA, M. and BENTON, M. J. 2011. Resetting the evolution of marine reptiles at the Triassic-Jurassic boundary. *Proceedings of the National Academy of Sciences*, **108**, 8339–8344.

TSAI, H. P. and HOLLIDAY, C. M. 2011. Ontogeny of the alligator cartilago transiliens and its significance for sauropsid jaw muscle evolution. *PLoS One*, **6**, e24935.

VENDITTI, C., MEADE, A. and PAGEL, M. 2011. Multiple routes to mammalian diversity. *Nature*, **479**, 393–396.

WAINWRIGHT, P. C. 2007. Functional versus morphological diversity in macroevolution. *Annual Review of Ecology Evolution & Systematics*, **38**, 381–401.

—— and PRICE, S. A. 2016. The impact of organismal innovation on functional and ecological diversification. *Integrative & Comparative Biology*, **56**, 479–488.

WALMSLEY, C. W., SMITS, P. D., QUAYLE, M. R., McCURRY, M. R., RICHARDS, H. S., OLDFIELD, C. C., WROE, S., CLAUSEN, P. D. and McHENRY, C. R. 2013. Why the long face? The mechanics of mandibular symphysis proportions in crocodiles. *PLoS One*, **8**, e53873.

WILLIAMS, M., BENTON, M. J. and ROSS, A. 2015. The Strawberry Bank Lagerstätte reveals insights into Early Jurassic life. *Journal of the Geological Society*, **172**, 683–692.

WILLS, M. A., BRIGGS, D. E. and FORTEY, R. A. 1994. Disparity as an evolutionary index: a comparison of Cambrian and Recent arthropods. *Paleobiology*, **20**, 93–130.

WITMER, L. M. 1995. The extant phylogenetic bracket and the importance of reconstructing soft tissues in fossils. 19–33. *In* THOMASON, J. J. (ed.) *Functional morphology in vertebrate paleontology*. Cambridge University Press.

WROE, S. and MILNE, N. 2007. Convergence and remarkably consistent constraint in the evolution of carnivore skull shape. *Evolution*, **61**, 1251–1260.

YOUNG, M. T., BRUSATTE, S. L., RUTA, M. and DE ANDRADE, M. B. 2010. The evolution of Metriorhynchoidea (Mesoeucrocodylia, Thalattosuchia): an integrated approach using geometric morphometrics, analysis of disparity, and biomechanics. *Zoological Journal of the Linnean Society*, **158**, 801–859.

—— —— BEATTY, B. L., DE ANDRADE, M. B. and DESOJO, J. B. 2012a. Tooth-on-tooth interlocking occlusion suggests macrophagy in the Mesozoic marine crocodylomorph *Dakosaurus*. *Anatomical Record*, **295**, 1147–1158.

—— —— DE ANDRADE, M. B., DESOJO, J. B., BEATTY, B. L., STEEL, L., FERNANDEZ, M. S., SAKAMOTO, M., RUIZ-OMENACA, J. I. and SCHOCH, R. R. 2012b. The cranial osteology and feeding ecology of the metriorhynchid crocodylomorph genera *Dakosaurus* and *Plesiosuchus* from the Late Jurassic of Europe. *PLoS One*, **7**, e44985.

—— DE ANDRADE, M. B., ETCHES, S. and BEATTY, B. L. 2013. A new metriorhynchid crocodylomorph from the Lower Kimmeridge Clay Formation (Late Jurassic) of England, with implications for the evolution of dermatocranium ornamentation in Geosaurini. *Zoological Journal of the Linnean Society*, **169**, 820–848.

ZAPATA, U., METZGER, K., WANG, Q., ELSEY, R. M., ROSS, C. F. and DECHOW, P. C. 2010. Material properties of mandibular cortical bone in the American alligator, *Alligator mississippiensis*. *Bone*, **46**, 860–867.

ZVERKOV, N. G., FISCHER, V., MADZIA, D. and BENSON, R. B. 2018. Increased pliosaurid dental disparity across the Jurassic-Cretaceous transition. *Palaeontology*, **61**, 825–846.